MODEL PREDICTIVE CONTROL OF BUILDING ENERGY MANAGEMENT SYSTEMS IN A SMART GRID ENVIRONMENT

By

Jeremy Dobbs

A THESIS

Submitted in partial fulfillment of the requirements for the degree of

MASTER OF SCIENCE

In Mechanical Engineering

MICHIGAN TECHNOLOGICAL UNIVERSITY

2015

This thesis has been approved in partial fulfillment of the requirements for the Degree of MASTER OF SCIENCE in Mechanical Engineering.

Department of Mechanical Engineering – Engineering Mechanics

Thesis Advisor: *Dr. Mahdi Shahbakhti*

Committee Member: *Dr. Lucia Gauchia*

Committee Member: *Dr. Sumit Paudyal*

Department Chair: *Dr. William W. Predebon*

Table of Contents

Acknowledgement

I would like to first thank my advisor, Dr Mahdi Shahbakhti, for his understanding, encouragement, and patience throughout the thesis process. I would like to thank my friends and family for their support through my time at Michigan Tech. Finally I would like to thank my fiancee Sarah Hubbell continuing for her love and support.

List of Figures

List of Tables

Nomenclature

HVAC	Heating, Ventilation and Air Conditioning
MPC	Model Predictive Control/Controller
$\dot{Q}_{cond}$	Rate of heat transfer by conduction (J/s)
k	Conductive coefficient of heat transfer ($W/m.K$)
A	Surface area available for transfer of heat (m^2)
x_{th}	Thickness of layer available for conduction of heat (m)
$\frac{dT}{dx}$	Temperature change with respect to change in thickness of layer (x)
$\dot{Q}_{conv}$	Rate of heat transfer by convection (J/s)
h	Convective coefficient of heat transfer
$\dot{Q}_{emit}$	Rate of heat transfer by radiation (J/s)
ε	Emissivity of radiating surface
σ	Stefan-Boltzmann constant ($5.67\times10^{-8}\frac{W}{m^2.K^4}$)
T_{emit}	Temperature of a radiation emitting surface (K)
$\dot{E}_{in}$	Rate of heat energy in (J/s)
$\dot{E}_{out}$	Rate of heat energy out (J/s)
$\frac{dE}{dt}$	Rate of change of heat energy
RC	Resistance-capacitance
I	Current in electrical circuit (Amp)
V_1, V_2	Voltages (V) at points 1 and 2 respectively in an electrical circuit
R	Resistance of an electrical circuit (Ω)
T_1, T_2	Temperatures at points 1 and 2 respectively (K)

C	Heat storage capacity $(J/kg.K)$
j	Wall $(where\ j = 1,2,3,4)$
C_p	Specific heat capacity of air $(J/kg.K)$
T_s	Temperature of air supplied by HVAC to a room (K)
T_r	Temperature of room air (K)
T_{wj}	Internal Temperature (K) of wall j
T_{dj}	Temperature (K) outside wall j
T_{d4}	Temperature outside of window (K)
$R_{wj_{in}}$	Thermal resistance of internal part of wall j (K/W)
$R_{wj_{out}}$	Thermal resistance of external part of wall j (K/W)
R_{win}	Thermal resistance of window (K/W)
R_j	Density $(\frac{kg}{m^3})$ of wall j
R_i	Density of inner three walls $\frac{kg}{m^3}$
R_o	Density of outer wall $\frac{kg}{m^3}$
ρ_a	Density of air $(\frac{kg}{m^3})$
Vol_r	Volume of room (m^3)
COP	Coefficient of performance of heat pump
A_{win}	Area of window (m^2)
Th_w	Thickness of window glass (m)
K_w	Conductivity of window glass $(W/m.K)$
R_i	Density of inner three walls of a room $(\frac{kg}{m^3})$
R_o	Density of outer wall of a room $(\frac{kg}{m^3})$
k_j	Conductivity $(W/m.K)$ of wall j
K_i	Conductivity of inner three walls of a room $(W/m.K)$
K_o	Conductivity of outer wall of a room $(W/m.K)$
h_{in}	Convection coefficient of inner three walls of a room $(W/m^2.K)$
h_o	Convection coefficient of outer wall of a room $(W/m^2.K)$
L_j	Thickness (m) of wall j
L_i	Thickness (m) of inner three walls
L_o	Thickness (m) of outer wall

C_w	Wall specific heat capacity $(J/kg.K)$
C_{wj}	Heat storage capacity (J/K) of wall j
C_r	Heat storage capacity of room (J/K)
A_{wj}	Surface area (m^2) of wall j
$\dot{m}$	Mass flow rate of air into a room from the heat pump fan $(\frac{kg}{sec})$
N	Time horizon
$T_{r_{lb}}^k$	Lower bound temperature (K) for room air temperature for k^{th} hour
$T_{r_{ub}}^k$	Upper bound temperature (K) for room air temperature for k^{th} hour
ε_{lb}	Slack variable for lower bound of room temperature
ε_{ub}	Slack variable for upper bound of room temperature
ρ	Penalty on room air temperature bounds
P_r	Dynamic pricing of electricity per MWh ($/MWh)
α	Weight on price in objective function
BEMS	Building energy management system
SOC	Battery State of Charge
P_{charge}	Power Charging Battery (W)
$P_{Discharge}$	Power Discharging Battery (W)
V	Voltage across battery (V)
C_B	Capacity of Battery (A-hr)
LF	Load Factor
β	Weight on Load Factor in Optimization
γ	Fan Power Coefficient

Abstract

Buildings are a major source of energy consumption. In the United States, buildings are responsible for more than 70% of all power consumption. Over 40% of this building power consumption is from the Heating, Ventilation, and Air Conditioning (HVAC) systems. Modern technologies such as building Energy Storage Systems (ESS), renewable energy sources, and advanced control algorithms allow for so-called Smart Buildings to increase energy efficiency. Smart Buildings further benefit from existing in a Smart Grid environment, where information such as pricing and anticipated power load is sent over two way communitcation between the grid operator and the power consumer.

The traditional control systems for these HVAC systems are often simple and do not exploit the principles of optimal control. This study applies Model Predictive Control (MPC) and ESS to the problem of controlling a Smart Building in a Smart Grid environment.

Simulations are performed for various optimal control objective functions. These objectives include price minimization, energy minimization, and an introduced Building to Grid (B2G) index optimization. The B2G optimization aims to both decrease the price of power for the consumer while avoiding large spikes in power consumption to maintain a steady load profile which benefits the grid operator. The results show that MPC has potential for large performance increases in Building Energy Management, while meeting the constraints for B2G integration.

Chapter 1

1 Introduction

Increasing the efficiency of energy consuming systems is an important issue in our increasinly energy-conscious world. Buildings are a major energy comsuming sector, accounting for more than 70% of the power consumption in the United States[1]. Of this, 40% of bulding power consumption is due to the Heating, Ventilation, and Air Conditioning (HVAC) system. This large section of power consumption has been a topic of active research into ways to increase the energy efficiency and reduce emissions by employing advanced technology and control techniques.

1.1 Smart Building Case Studies

A building that takes advantage of these emerging technologies is referred to as a *smart building*. Smart buildings may include advanced Building Energy Management Systems (BEMS), renewable energy sources such as solar and wind power, and Energy Storage Systems (ESS) such as stationary batteries and thermal storage. The BEMS can have many features which contribute to the building's performane. The focus of this thesis will be on designing BEMS control software which improves the performance of the building's HVAC system.

Additionally, studies have applied the BEMS towards sceduling applicance power loads, and controlling the building lighting load based on occupancy modeling. This is because the HVAC system is both a relatively large power load, and is controllable.

Tashtoush et al [2] introduced a component-based model for the control of an HVAC system. The model consists of the energy use of the heating coil, humidifier, fan, mixing box, cooling and dehumidifying coils, and the energy loss through both the ducts and the room the HVAC operates in. The energy use in heating the room is modeled to be dependent on only the room temperature, wall inner temperature, and humidity. The control algorithm developed had the goal of keeping temperature constant while the outdoor temperature, lighting, and occupancy of the room varied.

Fong et al [3] developed a component-based model of an air conditioning system. Their model describes mathematical models for the energy use of the chiller and the cooling coil. These models are based both on the physical properties of the components, and their nominal efficiency. The model was used in the genetic evolutionary optimization to develop an energy efficient control scheme.

Muratori et al [4] also developed a physics-based model for HVAC power consumption. Their model allows of the building to either use an all-electric heating system, or have an electrical fan, which circulates heat generated by a furnace. The power consumption for the fan is modeled separately from the heat generation. The heat transfer in the system is described with a simple thermodynamic model, where heat can move between the HVAC, building, and the environment. The power consumption is based on the model for the fan, and the model for the electric heating system.

Laio et al [5] developed a physical building model for estimating the indoor temperature. The model predicted the temperature based on the thermal properties of the HVAC system (including a water heated radiator) and building components, the power supplied to the HVAC system, and weather conditions.

Cai et al [6] developed a component model-based optimization for the power consumption of the condenser water loop in an HVAC system. The power consumption is the sum of the power consumptions of the chillers, pumps, and fans. The model uses the nominal specifications (power consumption, heat capacity) of the components along with adjustment factors, which account for the actual properties when the system is not running at maximum load or ideally. A genetic algorithm optimization is performed on the model to find an optimal control strategy.

Risbeck et al [7] controlled a building combined heating and cooling system using Mixed Integer Linear Programming (MILP). The model included binary on-off states and multivalue discrete states for the operator of each component. The results were compared to a Linear Programming (LP) approach.

1.2 Smart Grid Case Studies

The impact that a smart building has on energy efficieny can further increase by incorporating the building into a smart grid. In a smart grid, information can be sent through two way communication between the power grid distributor and the consumer.

One beneficial concept incoporated with the smart grid is *dynamic pricing*. With dynamic pricing, the price that consumers pay for electricity is dependent on the demand. During peak hours where the demand is high, the price is high. During off peak hours where the demand on the grid is low, the price is low.

Dynamic pricing is intended to incentize consumers to balance the power load. By making the dynamic pricing available to the consumer, the BEMS can shift the building's scheduable power loads to decrease the price of the consumer. Loads that can be scheduled, such as the HVAC and some applicances, can have the majority

of the load during hours where the price is low. This is advantageous for both the grid operator and the consumer. The consumer can decrease the cost of the energy they need. The grid operator will have a more balanced load as some of the load is scheduled to off peak hours.

Samadi et al [8] considered a smart grid with two way dynamic pricing communication. The model used a real time pricing model which showed benefits for both the consumer and energy provider.

Nyeng and Ostergaard [9] tested their controller with both a radiative space heater and a water tank heating system. They used both systems to heat a scale model room, and compared the cost savings for a constant temperature thermostat to their model, using both forecasted and actual pricing data from a Danish utility company. They found that, with both heaters, savings of more than 7% in cost occurred. The standard deviation in the temperature was found to be higher when using their price varying control model than without price response.

Lu et al [10] considered ways of balancing the grid load using HVAC control. They considered a model for residential HVAC systems. The study considered the ability to use HVAC systems for ancillary grid services. Kim et al[11] proposed a model for frequency regulation to regulate energy from unpredictable renewable resources in a smart grid. Hirata et al[12] proposed a real-time pricing model for the smart grid which increased grid stability.

1.3 Model Predictive Control for HVAC systems

Model predictrive control (MPC) can be used to benefit the performance of the building's HVAC system. The advantage of MPC is that it allows the system to anticipate future changes and disturbances to the system dynamics. It also allows the system to adjust to any disturbances over time.

MPC has been used in previous building HVAC control studies. Haung et al [13] combined linear MPC with a neural network for building HVAC control. The neural network handled nonlinearities present in the building model. The hybrid model was tested and validated on a commericial building.

Vasak et al [14] presented an MPC algorithm for controlling the HVAC system of a residential household. The resistor capacitor (RC) thermal model is used to model the building.

Maasoumy et al[15] presented a building thermal model which used Kalman filtering to update model parameters over time to account for modeling uncertaininty and disturbances. The model was validated using data from a Michigan Tech office building. The model was then used for MPC and Robust Model Predictive Control (RMPC) control simulations.

Razmara et al[16] performed bidirectional optimization of a building HVAC system in a smart grid. The study introduced the building to grid (B2G) index to find a balanced optimization which both reduced grid peak load and HVAC run cost. The control algorithm included options for curtailing load based on the operational limits of the smart grid. The results found 25% savings when compared to an unoptimized rule-based controller (RBC).

Maasoumy et al [17] presented an MPC approach for controlling the HVAC system of a university campus building. The model focuses on controlling the mass flow rate of the air in the HVAC system.

Wei et al [18] considered the opitimization of a smart building that included optimization of the HVAC system, PHEV charge scheduling, and battery energy storage. MPC was used to formulate the control algorithm. Peak energy demand and overall energy cost were decreased through use of battery storage and MPC.

Galus et al [19] studied utilizing MPC to control a smart grid with PHEVs and building HVAC systems. Nowak et al [20] compared MPC to using a fuzzy logic control algorithm when performing optimal control of an HVAC system.

Halvgaard et al [21] presented a MPC algorithm for smart building control. The model was developed for a residential building with floor heating systems. The controller used dynamic pricing information to shift power loads to times with low energy cost. Rehrl et al [22] used MPC along with feedback linearization to control a component level model of an HVAC system.

Kelman et al [23] used MPC to study a nonlinear HVAC control problem. A problem formulation for the nonlinear system is presented. Local optima were found to the nonlinear optimization problem.

Ma et al [24] showed a comparison of a simulated and experimental MPC implemetation. The MPC logic to control an HVAC system was tested through simulation and then validated through experimental implementation on a university campus building.

1.4 Technical Scope of this Thesis

The studies available in current literature have studied many aspects of smart building control and interaction with the smart grid. However, there are shortcomings in the literature which this thesis will address. The objectives of this thesis are to establish the technical base required to formulate the building MPC problem, then fill the following gaps in the current scientific literature.

Various studies have designed MPC algorithms for building HVAC systems. However, to the author's knowledge, very little research has compared the relative effectiveness of different control actuators for the same building HVAC system. Thie study will compare controlling the HVAC system by varying the air mass flow

rate, supply air temperature, and a combination of mass flow rate and supply temperature. Scenarios with both dynamic pricing and flat pricing will be considered. Additionally, the effect of adding battery energy storage to the building HVAC system is presented.

This study will also build upon previous research [16] covering integrating smart building control into a smart grid. Work on B2G integration is currently limited. This study will build upon the results in [16] to perform B2G control with a comparison of different control actuation modes for the HVAC system, and comparisons of the B2G objective function to other grid and consumer focused objective functions.

The scope of this work will encompass simulations based upon a Michigan Technological University office building. The physical model is based upon and validated with this building. Then, MPC problems are defined using this model as the plant.

1.5 Organization of Thesis

The organization of this thesis will now be outlined. The preceding chapter has introduced the concept of smart control of smart buildings in a smart grid environment. The next chapter will introduce the physical theory and mathematical techiqnues required to simulate MPC for a building's HVAC system. In Chapter 3, building HVAC energy optimization results will be presented, comparing mutiple control cases for the system. Chapter 4 will introduce aspects of the smart grid into the control simulation, and strike a balance between optimizing the benefit for the single building and the grid as a whole. Finally, Chapter 5 will offer conclusions on the study and potential paths for future work

Chapter 2

2 Modeling and Optimization

2.1 Building Thermal Model

The goal in this chapter is to develop the mathematical tools required to model and control the HVAC system of a smart building. First we will develop the physical model for heat transfer in the building.

The building being modeled is Michigan Technological University's Lakeshore Center. The building is used for administrative offices and offices leased to local businesses. The Lakeshore Center was chosen for this study because its construction and inhabitance schedule are typical for an office building. Additionally, the recorded database of the building's temperature and power consumption was available through the Building Energy Management System (BEMS) for use as model validation.

Figure 2.1: Lakeshore Center- Building Test Bed in this Thesis

A physics-based model for heat transfer in this building will be developed. The model will be based on fundamental heat conduction, convection, and radiation equations:

$$\dot{Q}_{cond} = \frac{T_1 - T_2}{\frac{x_{th}}{kA}} \tag{2.1}$$

$$\dot{Q}_{conv} = \frac{T_1 - T_2}{\frac{1}{hA}} \tag{2.2}$$

$$\dot{Q}_{rad} = \varepsilon\sigma A T_{rad}^4 \tag{2.3}$$

Here $\dot{Q}_{cond}$ is the conductive heat flow, T_1 is the temperature of one node in the thermal model, T_2 is the termperature of the adjacent thermal node, A is the surface area, k is the conductive heat transfer coefficient, h is the convective heat transfer coefficient, x_{th} is the thickness of the material, ε is the emissivity of the radiating surface, σ is the Stefan-Bltzmann constant, $\dot{Q}_{rad}$ is the radiative heat flow, and T_{rad} is the temperature of the radiating surface.

The conductive and convective resistances for a thermal circuit can be given by $\frac{x_{th}}{kA}$ and $\frac{1}{hA}$.

Using these fundamental equations, the convection of heat through the air in the rooms, and the conduction of heat through the walls and windows, will be modeled. The heat transfer model will consider a typical room in the Lakeshore center. Other rooms surround three sides of the room. The fourth wall is adjacent to the outside and exposed directly to outdoor temperatures. This room is serviced by a heat pump HVAC system, and an energy model for this HVAC system will also be developed. This single room will be scaled up to model a building with 30 rooms.

Figure 2.2 shows a schematic of the thermal model. The room temperature is dependent on the surrounding room temperatures, the outdoor temperature, and the thermal properties of the walls and windows.

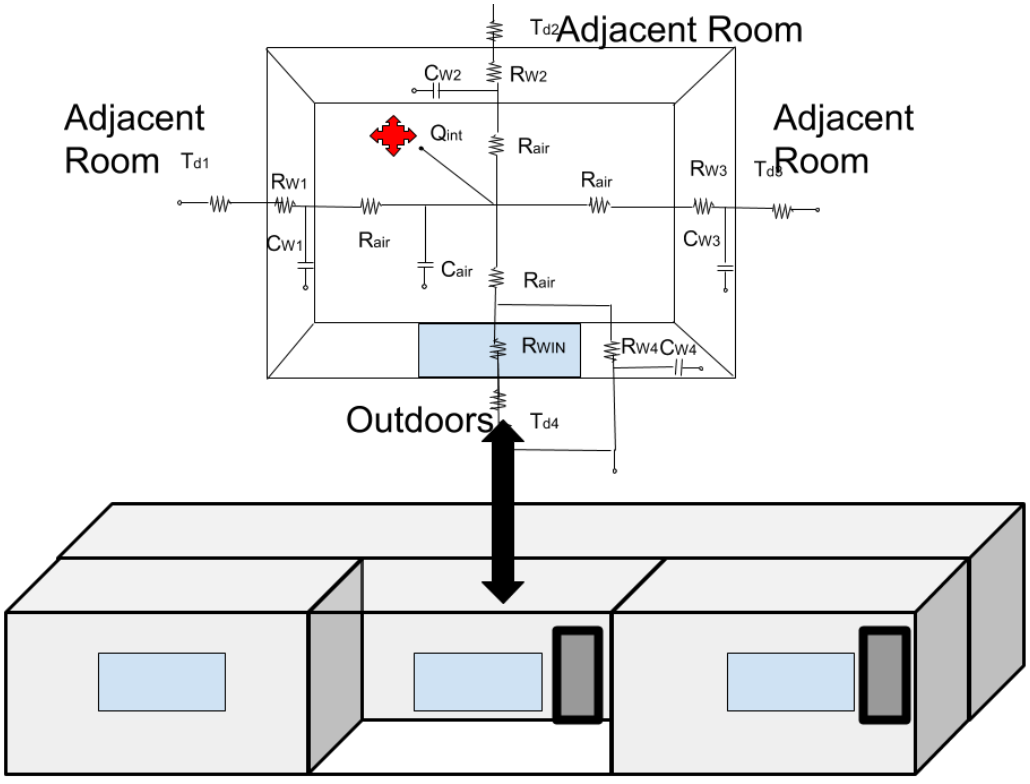

Figure 2.2: System schematic. The model represents the heat transfer of a room in the Lakeshore Center. Adapted from [15].

The model type is referred to as an RC thermal model. The model is directly analogous to a Resistor-Capacitor (RC) electrical circuit. Each component of the system (walls, air in the rooms) has a thermal resistance and capacitance, which dictates the dynamics of how heat flows through the building. Once these material properties are known, a system of differential equations can be written which describes the heat transfer over time. The RC thermal model is commonly used for modeling heat transfer in buildings.

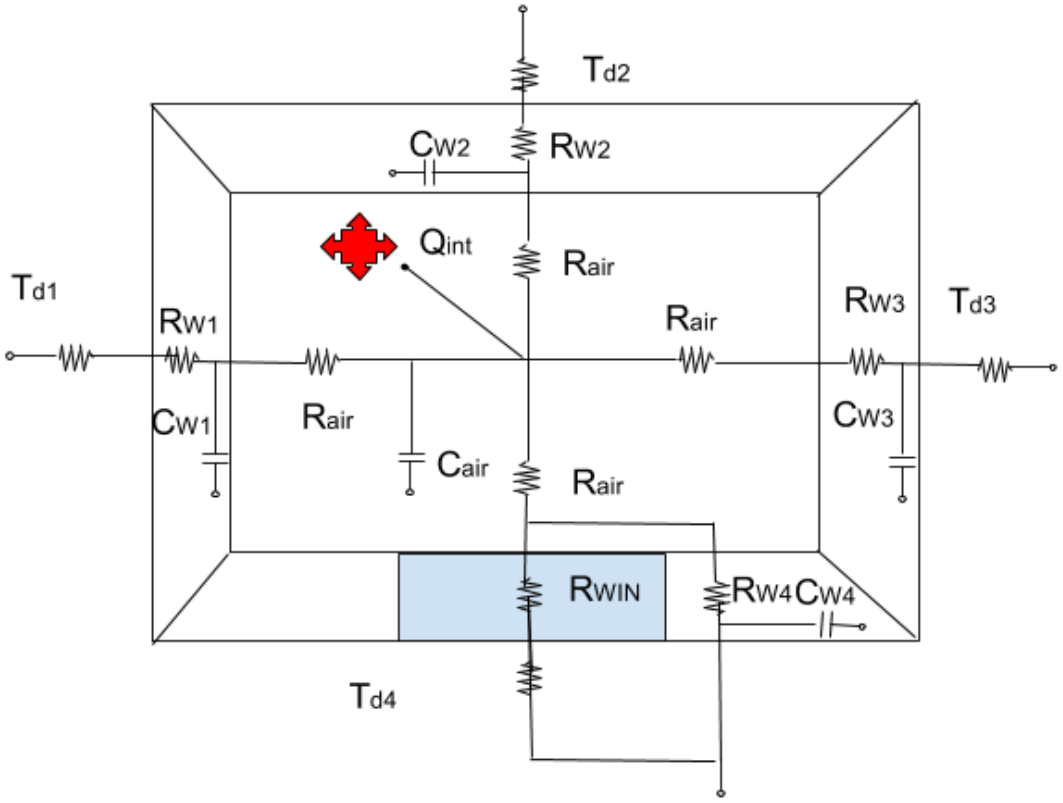

Figure 2.3: RC heat transfer model. Thermal resistance and capacitance of each wall, room, and window combine to form a thermal circuit. Adapted from [15].

The heat transfer through any material can be modeled by considering the thermal resistance and capacitance of the materials. The model is based on the thermal resistance and capacitance of the walls and rooms of the building. For multi-paned windows and layered walls, the thermal properties of each layer are combined in series to give an overall thermal resistance and capacitance. The heat transfer through a wall is:

$$C_{wi,j}\frac{dT_{wi,j}}{dt} = \sum_{k\in N_{\{w\,i,j\}}}\frac{T_{rk}-T_{wi,j}}{R_{wi,j_{in}}} \tag{2.4}$$

Here $C_{wi,j}$ is the specifice heat capacity of the wall between rooms *i* and *j*, $T_{wi,j}$ is the temperature of the wall between rooms *i* and *j*, T_{rk} is the temperature in room *k*, and $R_{wi,j}$ is the thermal resistance of the wall between rooms *i* and *j*.

The rate of temperature change is based on the adjacent node temperatures, and the resistance and capacitance of the wall. This is the heat transfer model that will be

used as the basis of the dynamic model for the control model. The additional pieces that must be added into the model are the inputs from the HVAC system.

2.2 HVAC model

In this section the energy model for the HVAC system will be developed. This will complete the model for heat transfer in the Lakeshore Center.

The Heating system in the Lakeshore center is a ground source heat pump (GSHP). A GSHP uses thermal energy from below ground. It takes advantage of the relatively constant temperature of the ground below a few meters. During cold months, heat is extracted from the relatively warm ground by the heat pump. Figure 2.4 shows a schematic of the system.

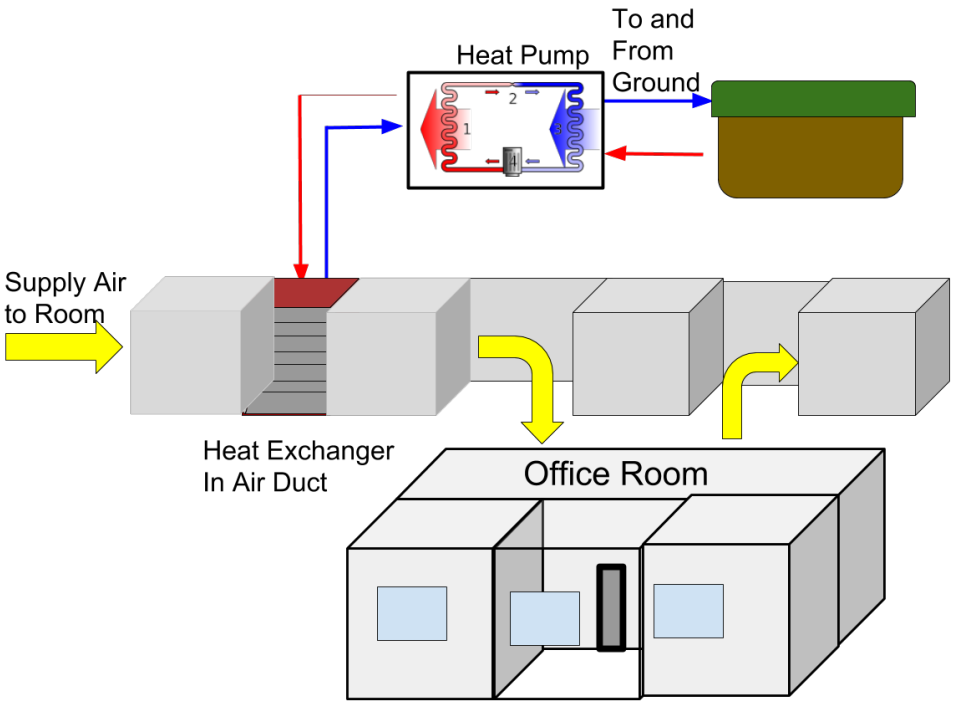

Figure 2.4: HVAC system setup. The GSHP supplies heat, which heats air, which is then circulated into the room by a blower in the HVAC duct. Adapted from [15].

The GSHP supplies hot water to a heat exchanger in the ventilation duct. The supply air temperature is increased by passing through the heat exchanger, and then into the room to supply heat.

For control purposes a simple model will be adopted for the electrical energy consumption of the HVAC system. This model is based on the nominal coefficient of performance (COP) of the system. The energy consumption of the HVAC system is modeled as

$$COP * \dot{m}_{r_i} c_a \left(T_{s_i} - T_{r_i}\right) \tag{2.5}$$

Here COP is the coefficient of performance, $\dot{m}_{r_i}$ is the mass flow rate of air from the HVAC system in room *i*, c_a is the specific heat capacity of the air, T_{si} is the supply air temperature from the HVAC system in room *i,* and T_{ri} is the air temperatuer in room *i.*

The room temperature is dependent on the surrounding room and outdoor temperatures, the internal wall temperatures, the thermal properties of the walls and windows surrounding the room, and the temperature of the air supplied by the HVAC system (supply temperature) and the mass flow rate of the air coming from the HVAC system. It also depends on any internal heat sources within the room. By combining Equations *2.4* and *2.5,* the model for temperature in room *i* with an HVAC system is:

$$C_i^r \frac{dT_{r_i}}{dt} = \sum_{k \in N_{r_i}} \frac{T_k - T_{r_i}}{R_{i,k_i}} + \dot{m}_{r_i} c_a (T_{s_i} - T_{r_i}) \tag{2.6}$$

Depending on the control mode of the HVAC system, the mass flow rate, the supply temperature, or both may be variable. The model will consider a building with 30 zones, which are each serviced by an HVAC system.

These differential equations describe the behavior of the system. With the physics based heat transfer model and energy consumption model, we can develop a system of differential equations for the heat transfer dynamics of the building. In order to develop the control model, the differential equations will be translated into a state space equation.

2.3 State Space Model

For control purposes the model is converted into a set of state space equations. We define the state equation:

$$x = [x_1, x_2, x_3, x_4, x_5] = [T_{r1},\ T_{w12}, T_{w13}, T_{w14}, T_{w15}\ ]^T \tag{2.7}$$

Here x is the system state, T_{r1} is the room temperature, T_{w1j} is the wall temperature between node 1 and the adjacent nodes for *j={2,3,4,5}*.

Then, using equation (2.6) along with this state definition, the state space model is defined. Using standard techniques we find that the state model is:

$$\dot{x_1} = -4 * \frac{x_1}{C^w R^w} + \frac{2}{C^w R^w}(x_2 + x_3 + x_4 + x_5) + \dot{m}_{r_i} c_a \left(T_{s_i} - x_1\right)$$

$$\begin{aligned}
\dot{x_2} &= \frac{x_1}{C^w R^w} - \frac{2}{C^w R^w} x_2 + \frac{T_2}{C^w R^w} \\
\dot{x_3} &= \frac{x_1}{C^w R^w} - \frac{2}{C^w R^w} x_3 + \frac{T_3}{C^w R^w} \\
\dot{x_4} &= \frac{x_1}{C^w R^w} - \frac{2}{C^w R^w} x_4 + \frac{T_4}{C^w R^w} \\
\dot{x_5} &= \frac{x_1}{C_{51}^w R_{51_1}} - \left(\frac{1}{C_{51}^w R_{51_1}} + \frac{1}{C_{51}^w R_{51_5}}\right) x_5 + \frac{T_5}{C_{51}^w R_{51_5}}
\end{aligned} \tag{2.8}$$

Here C^w is the thermal capacitance of the inner walls, R^w is the thermal resistance of the inner walls, C_{51}^w is the thermal capacitance of the wall between the outside and the room, $R_{51_5}$is the thermal resistance of the wall between the outside and the room, and the remaining symbols are as previously defined.

Then by defining matrices with the appropriate dimension, the final state space model is

$$\dot{x} = Ax + Bu + Fd \tag{2.9}$$

$$y = Cx \tag{2.10}$$

where,

$$u = T_s \tag{2.11}$$

$$d = [T_{d1}, T_{d2}, T_{d3}, T_{d4}] \tag{2.12}$$

$$y = T_r \tag{2.13}$$

Here the terms in the disturbance vector d, T_d, are the temperatures of the adjacent zones. For full details of the state space model, see Appendix A.

The standard control model for this heat pump is to consider the supply air temperature as a control variable and the mass flow rate of the supplied air as a constant. This leads to the linear model presented in Equation 2.8. Alternatively, the supply temperature can be kept constant with a controllable mass flow rate. This problem formulation simply reverses the position of mass flow rate and supply temperature in the state space equation formulation.

Under mass flow rate control, the input vector is defined as:

$$u = \dot{m}_r$$

And the A matrix is adjusted appropriately.

In both of these situations, the system dynamics are linear. The dynamics can be formed into a system of linear equations. Finally, we can consider the case where both the mass flow rate and supply temperature of the HVAC system air supply are controllable. In this case, the system dynamics are nonlinear, which complicates the mathematical formulation and solution. Specifically, notice that the system state now depends on the product of two variable system inputs (the notable terms are bolded for emphasis):

$$\dot{x_1} = -4 * \frac{x_1}{C^w R^w} + \frac{2}{C^w R^w}(x_2 + x_3 + x_4 + x_5) + \boldsymbol{\dot{m}_{r_i}} c_a \left(\boldsymbol{T_{s_i}} - x_1\right)$$

Due to these products between control variables, this nonlinear control problem is more difficult to solve than the two previous problems, because it cannot be solved using standard Linear Programming (LP) techniques. A linear system of matrix equations such as Equation 2.9 cannot be defined for this system. A solver will be chosen for this study, which is capable of solving nonlinear programming (NLP) optimization problems.

2.4 Model Validation

The mathematical model that has been developed up to this point needs to be validated. If the model does not accurately represent the system dynamics, any simulation results using them may not be valid. The values of parameters used for this validation are shown in Table 2.1.

Table 2.1: Parameters for model validation

Parameter	Definition	Value
C_p	Specific heat capacity of air	1005 $J/kg.K$
ρ_{air}	Density of air	1.205 $\frac{kg}{m^3}$
COP	Coefficient of performance of HVAC heat pump	3.2
A_w	Area of window	3 m^2
T_w	Thickness of window glass	0.01 m
K_w	Conductivity of window glass	0.96 $W/m.K$
R_i	Density of inner three walls	240 $\frac{kg}{m^3}$
R_o	Density of outside wall	2000 $\frac{kg}{m^3}$
K_{in}	Conductivity of inner three walls	0.048 $W/m.K$
K_{out}	Conductivity of outside wall	0.72 $W/m.K$
h_{in}	Convection coefficient for inner three walls	5 $W/m^2.K$
h_o	Convection coefficient for outside wall	20 $W/m^2.K$
C_w	Heat storage capacity of walls	800 $J/kg.K$
A_{wj} $(where\ j = 1,3)$	Surface area of long inner wall	27.54 m^2
A_{wj} $(where\ j = 2)$	Surface area of shorter inner wall	22.95 m^2
A_{wj} $(where\ j = 4)$	Surface area of outer wall	19.95 m^2
L_{in}	Thickness of inner three walls	0.15 m
L_{out}	Thickness of outer wall	0.70 m
$\dot{m}_r$	Mass flow rate of air from the HVAC system	0.52 $\frac{kg}{sec}$

The model was validated using data collected from the Lakeshore Center. The Lakeshore Center's Building Management Software collects temperature data for all zones in the building and the temperature of air supplied by the HVAC system. The input temperature from the HVAC system and room temperature were measured over a one-week period. To validate the model, the same inputs were applied to the model and the system dynamics were simulated. The simulated and measured temperature profiles can be found in Figure 2.5.

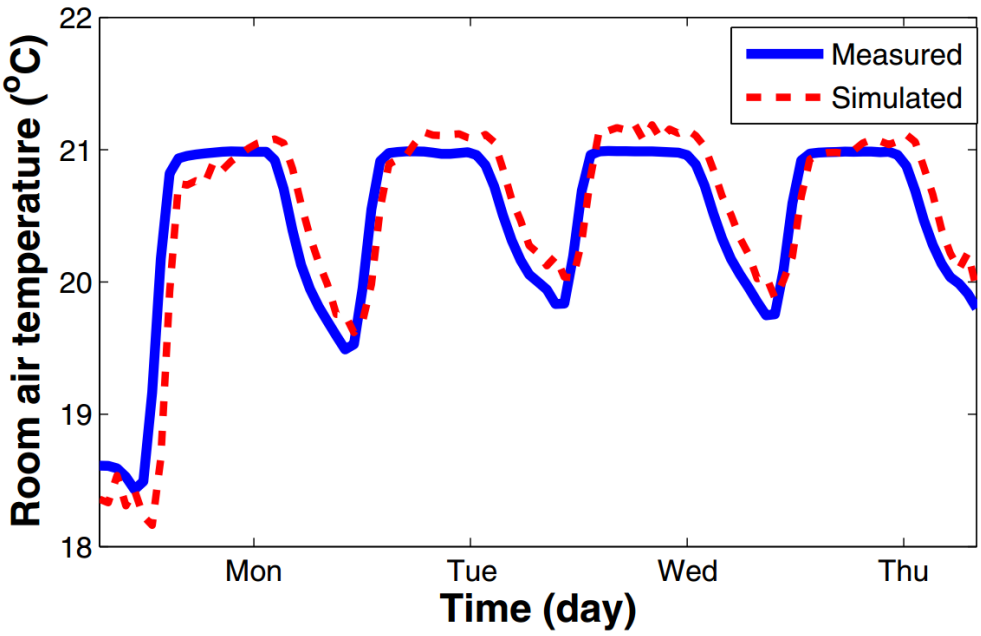

Figure 2.5: Validation of the building HVAC model. The temperature profile from the simulation closely matches the measured data.

The results in Figure 2.5 validate the system model. The simulated temperature profile is very similar to the measured values. The validated model can now be used to design the control algorithm.

2.5 Optimization and Optimal Control

The field of optimization is concerned with finding the minimum or maximum point of a function that satisfies a set of constraints. In optimal control, the goal is to choose control inputs for a dynamic system that optimize the value of a cost function. The theoretical basis for optimal control is based on the Calculus of Variations. A typical optimal control problem takes the form:

$$\min f(x) \tag{2.14}$$

$$s.t.\ g_i(x) \leq 0 \quad for\ i = 1, \dots, m \tag{2.15}$$

$$h_j(x) = 0 \quad for\ j = 1, \dots, n \tag{2.16}$$

$$x \leq 0\ or\ x \geq 0 \tag{2.17}$$

Here f(x) is the objective or cost function. h(x) and g(x) are constraints imposed on the problem. The constraints can take the form of equality or inequality equations that must be satisfied. The goal is to find the minimum of f(x) which is within these constraints. If no solution is found which satisfies the constraints, the problem is infeasible.

2.6 Model Predictive Control (MPC)

Model predictive control utilizes optimal control theory to implement a real-time controller. A typical optimal controller will predetermine the optimal solution offline; e.g., if the objective is to optimize the HVAC system's behavior over the next 24 hours, the optimal control problem will be solved at the beginning, and then implemented over the 24 hours. With MPC, the controller inputs are chosen in real time over the 24-hour period. This allows the controller to more easily adapt to any disturbances. Specifically, this study will utilize receding horizon control. Figure 2.6 illustrates the receding horizon MPC concept.

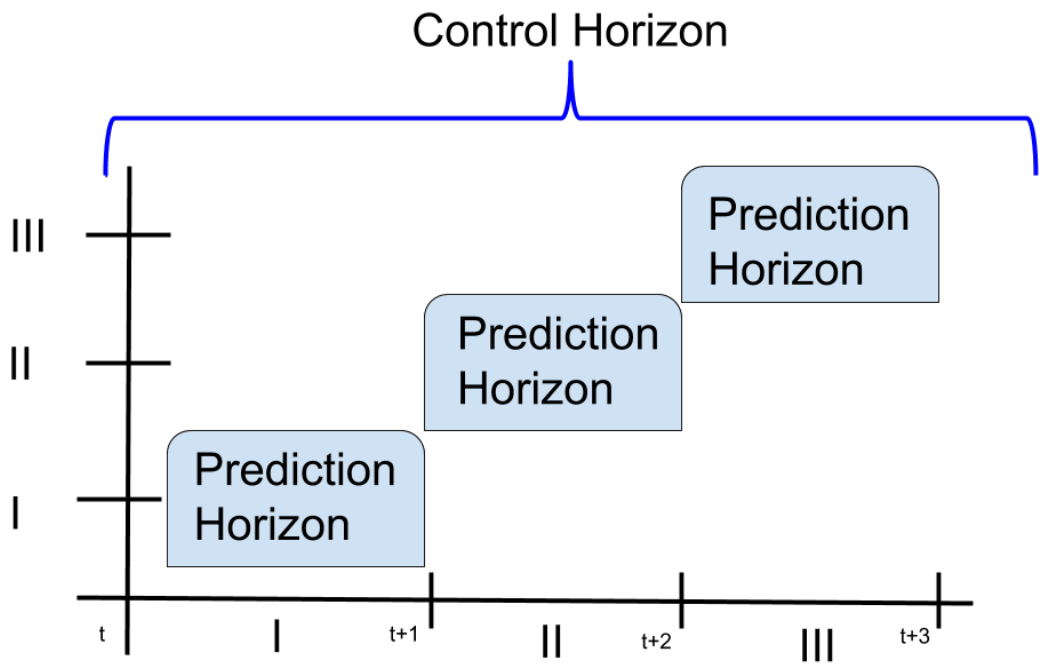

Figure 2.6: Receding Horizon Model Predictive Control. New Prediction Horizons are formed over the control domain. Adapted from [25].

Additionally, MPC allows for the controller to anticipate changes in the system dynamics and adapt accordingly. The controller is provided with some forecast of disturbances to the system, i.e., a weather forecast in the case of building HVAC control. The controller is using foreknowledge of the information when forming the optimal control problem, and thus can utilize it to find a more optimal solution.

An objective function and the problem constraints are formed over the prediction horizon. The optimal control problem is then solved, and the first input from the solution is applied. The system dynamics then iterate to the next time step. A new prediction horizon is formed and another optimal input is solved.

2.7 Battery Model

This section will develop a model for the dynamics of a battery used in conjunction with the HVAC system. The battery is used as an Energy Storage System (ESS), where energy can be stored by charging the battery and then the battery is discharged to power the HVAC system.

Here, an LG Chem 5kWh Air Cooled Battery from Michigan Tech's Energy Mechatronics Lab (EML) is used. The model is based on performance maps that are available for the battery. These maps dictate the maximum charge and discharge power achievable by the battery at a given state of charge (SOC) and temperature. The power maps are shown in Figure 2.7.

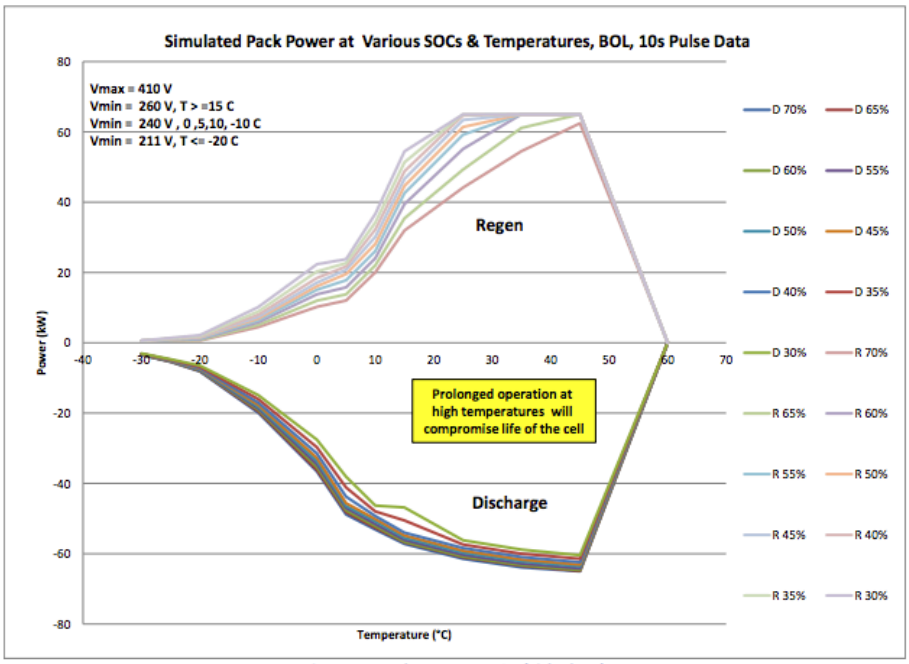

Figure 2.7: Power Map for LG Chem 5kWh Air Cooled Battery. Data from [26].

The maximum discharge and charge power of the battery is determined by the SOC of the battery. The SOC is calculated using the following difference equation [18]:

$$SOC_{t+k+1|t} = SOC_{t+k|t} + \frac{P_{charge} - P_{discharge}}{V\ C_B} \quad (2.18)$$

Here SOC is the state of charge, P_{charge} is the power charging the battery, $P_{discharge}$ is the power discharging from the battery, V is the voltage across the battery, and C_B is the capacity of the battery.

2.8 Numerical Methods

The control problems in this thesis will be solved using the YALMIP solver in MATLAB. YALMIP is a freely available toolbox for solving model predictive control problems in MATLAB. It has the advantage of simplifying the process of translating the formal mathematical statement of the optimization problem into MATLAB code. Details on YALMIP and its usage are available in [27].

The solver used in this study in YALMIP is the IPOPT solver. Since the control problem formulation is nonlinear when both supply temperature and mass flow rate are controlled, the solver must be able to solve nonlinear programming (NLP) optimization problems. The solver is able to solve NLP control problems. The IPOPT solver uses inner boundary value techniques to solve nonlinear control problems. More information on IPOPT is available in [28].

With the system modeling developed and the theory of the optimization problem reviewed, the energy optimization problem can now be formed and solved.

Chapter 3

3 Optimal Control of Building Energy Cost

Buildings account for over 70% of power consumption in the United States. Of this, over 40% is used by the buildings' Heating, Ventilation, and Air Conditioning (HVAC) system. Traditional HVAC control algorithms are often simple on-off or rule based controllers (RBC). Figures 3.1 and 3.2 show the simulated behavior of a building where the HVAC system has an RBC. The logic for the controller is the same is that used in Michigan Tech's Lakeshore Center.

The RBC used followed the following logic. When the temperature in the room was within the comfort bounds, the HVAC system supply air temperature was the same as the temperature of the air in the room and air was recirculated without heating. When the room air temperature was below the allowed bounds, the supply air temperature would increase to 32 C.

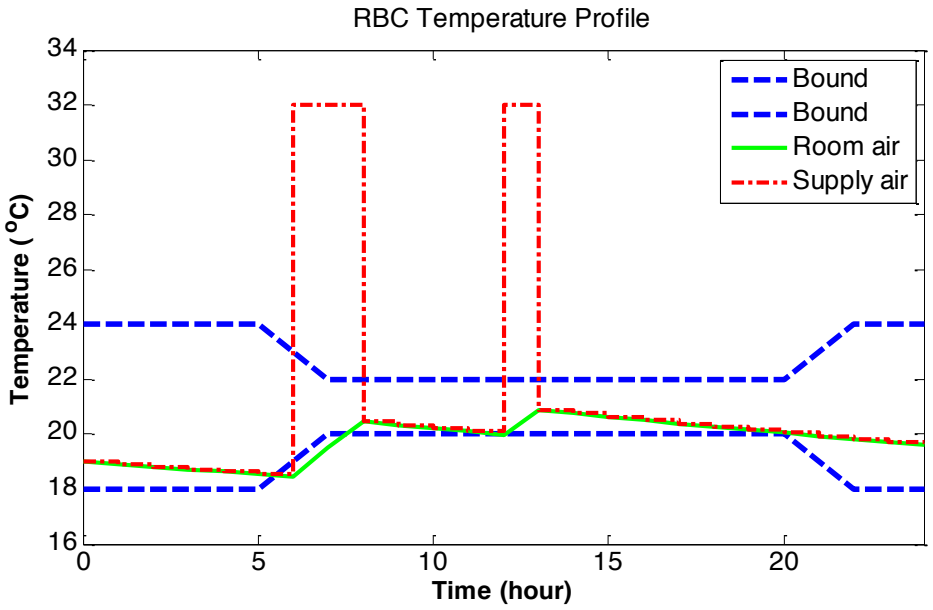

Figure 3.1: Room Temperature Profile with RBC.

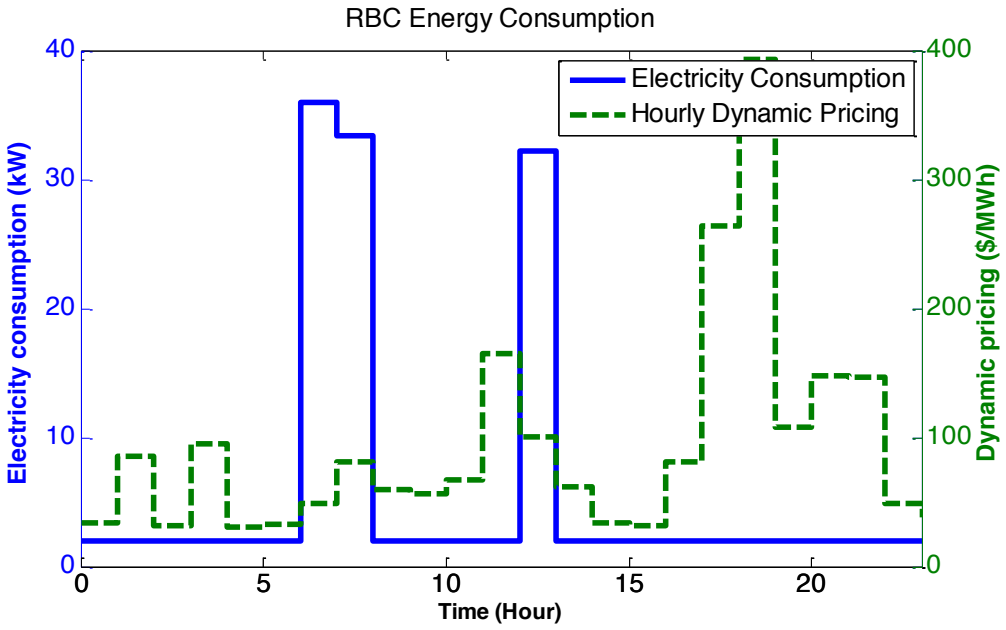

Figure 3.2: Electricity Consumption with RBC.

Rule Based Control is simple to implement and can keep the room's temperature within constraints. But, there is a large potential for increasing the systems performance. Some shortcomings of the method can be seen in Figures 3.1 and 3.2. In Figure 3.1, the room is heated more than necessary to stay within the desired temperature constraints, which means more energy is used then is necessary. Additionally, the controller does not account for the hourly variations in the cost of the energy used. In Figure 3.2, the large spikes in electricity consumption do not correspond with hours with the lowest energy cost. In summary, neither the cost nor the amount of energy used is optimized.

By using optimal control these shortcomings of the RBC can be overcome. Specifically, the goal in this chapter is to develop an optimal Model Predictive Control (MPC) algorithm for the Building Energy Management System (BEMS).

3.1 Optimal Control Problem Formulation

As explained in Chapter 2, the goal in optimal control is to optimize an objective function while staying within given constraints. In the case of building HVAC control, the objective will be to minimize the price of running the HVAC system. The constraints are the upper and lower bounds on room temperature to maintain comfort, constraints caused by the capabilities of the HVAC system, and the system dynamics.

As previously explained in Chapter 2, MPC is a practical way to implement optimal control on a dynamic system subject to disturbances. Previous studies have utilized MPC algorithms for building energy management.

The optimization problem can be stated as:

$$\min_{I_e,\overline{\epsilon}\underline{\epsilon}}\{(I_e \cdot P_{Dyn}^T) + \rho(|\overline{\epsilon}_t|_1 + \left|\underline{\epsilon_t}\right|_1)\} \tag{3.1}$$

subject to:

$$x_{t+k+1|t} = A\, x_{t+k|t} + Bu_{t+k|t} + Ed_{t+k|t} \tag{3.2}$$

$$y_{t+k|t} = C\, x_{t+k|t} \tag{3.3}$$

$$\underline{u} \leq u_{t+k|t} \leq \overline{u} \tag{3.4}$$

$$\underline{\delta u} \leq u_{t+k+1|t} - u_{t+k|t} \leq \overline{\delta u} \tag{3.5}$$

$$\underline{T}_{t+k|t} - \underline{\varepsilon}_{t+k|t} \leq y_{t+k|t} \leq \overline{T}_{t+k|t} + \overline{\varepsilon}_{t+k|t} \tag{3.6}$$

$$\underline{\varepsilon}_{t+k|t}, \overline{\varepsilon}_{t+k|t} \geq 0 \tag{3.7}$$

Here P_{Dyn}^T is the hourly dynamic price of electricity, ρ is the weight on the soft constraint penalties from the slack variables, and $\overline{\epsilon}_t$ and $\underline{\epsilon_t}$ are the upper and lower slack variables. Equations 3.2 and 3.3 present the system dyanmics as defined in Section 2.3. $\underline{u}$ and $\overline{u}$ are the lower and upper constraints on the input vector u. $\underline{\delta u}$ and $\overline{\delta u}$ are constraints on the hourly change in the input vector u.

The objective function is defined using the Energy Index (I_e):

$$I_e = \sum_{t=0}^{24}\left[P_h(t) + P_c(t) + P_f(t)\right] \tag{3.8}$$

Where

$$P_h(t) = \dot{m}_i^r(t)c_{p,air}\left[T_h(t) - T_{r_i}(t)\right] \tag{3.9}$$

$$P_c(t) = \dot{m}_i^r(t)c_{p,air}[T_{r_i}(t) - T_c(t)] \tag{3.10}$$

$$P_f(t) = \gamma(\dot{m}_i^r)^3 \tag{3.11}$$

P_h is the power consumed to heat the room, P_c is the power consumed to cool the room, and P_f is the power consumed by the fan in the HVAC system. Here, γ is the power coeffient for the fan.

The equality constraints in the optimization problem are representative of the system dynamics. In order for the problem to be feasible, the state equations of the system dynamics must be true. In this way the system dynamics are implicitly considered by the optimization problem.

There are inequality constraints on the inputs. Some of the inequality constraints are due to the physical limitations of the HVAC system. These are the upper constraints and the constraint on the difference between consecutive inputs. The lower constraint on the input, which determines the minimum allowable mass flow rate of air in the optimization problem, is set to meet the ventilation requirements for the building. The ventilation constraint $\dot{m}_{min}$ is implemented to ensure the Air Changes per Hour required by ASHRAE standards are met.[29]

The constraint on the output (room temperature) is to ensure comfort. The constraints are based on ASHRAE standards for comfort. [29] The comfortable temperature range is tighter during the day when the office is occupied, and relaxed at night.

In order to ensure that the solver finds a feasible solution, slack variables are introduced to relax the comfort constraints [15]. In this way, the system is permitted to leave the comfort constraints if no feasible solution is available otherwise. A penalty term is introduced into the objective function using the slack variables.

Tuning the coefficient ρ on this term allows for a tradeoff between price and comfort.

The optimization problem is to minimize the cost of running the HVAC system with a time varying price P_{Dyn}^{T}. Dynamic pricing is a concept where the price of electricity varies over the course of the day based on demand. Hours with higher energy demands will have higher prices. This study assumes that these prices are set 24 hours ahead based on the predicted grid load. This 24-hour ahead pricing information can be leveraged by the controller to provide price savings to the building owner.

This general problem can be approached in different ways. The HVAC system in this building has two possible control variables: The mass flow rate of air into the room, and the temperature of the air supplied to the room. Both the mass flow rate and temperature can be varied to control the amount of heat supplied to the room. Three cases will be examined: (i) supply temperature control, (ii) mass flow rate control, and (iii) combined supply temperature and mass flow rate control. The system will be simulated using these three possible combinations of controls variables, and the results will be compared.

3.2 Price Minimization with Supply Temperature Control

The system was first simulated in supply temperature control mode. The mass flow rate of the HVAC system was set to a constant value and the heat supplied to the room was varied through varying the supply temperature of the heat pump.

The performance in supply temperature control mode was tuned. The cost of running the HVAC system varies depending on chosen mass flow rate set point. Too high and too low of a set point can increase the cost. Various set points were chosen and the system was simulated at each set point. The optimal mass flow rate is found through this tuning process. Figure 3.3 illustrates the results of this tuning process.

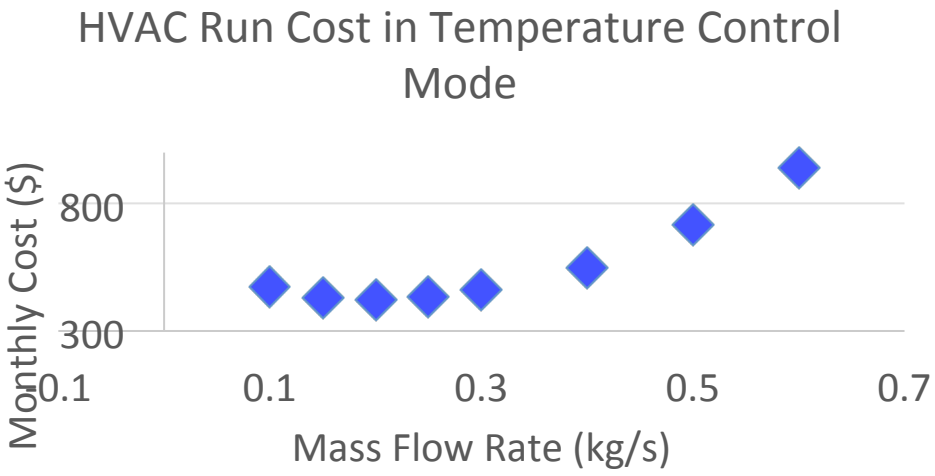

Figure 3.3: Tuning Curve for Supply Temperature Control. The Price is optimized for this mode when Mass Flow Rate is set to 0.2 kg/s.

The optimal set point for the mass flow rate was found to be 0.2 kg/s. The monthly cost to run the HVAC system increases if the mass flow rate is changed in either direction. The cost increases drastically as the mass flow rate is increased. This is because a large amount of air is being recirculated by the HVAC system even when very little heat is required by the room. The cost also increases if the mass flow rate is decreased. This is because the system's actuation is not strong enough when the mass flow rate is decreased.

The results of an optimal control simulation over 24 hours with the optimal mass flow rate set point is shown in Figure 3.4. These results show a few interesting

features of optimal price minimization. Some preheating occurs when prices are lower so that the actuation can be low during hours with higher prices. In general the room temperature stays close to the lower limit.

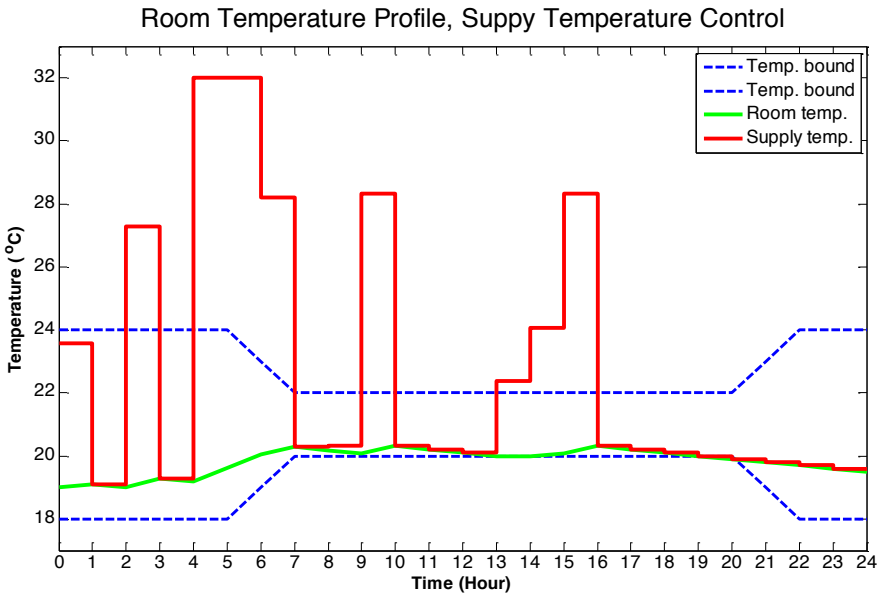

Figure 3.4: Temperature profile for supply temperature control case. ($\dot{m}^r$ =0.2 kg/s)

The control inputs for the HVAC are shown in Figure 3.5. The mass flow rate is set to 0.2 kg/s as chosen by the tuning process. The supply temperature shown is the input chosen as the solution to the MPC problem.

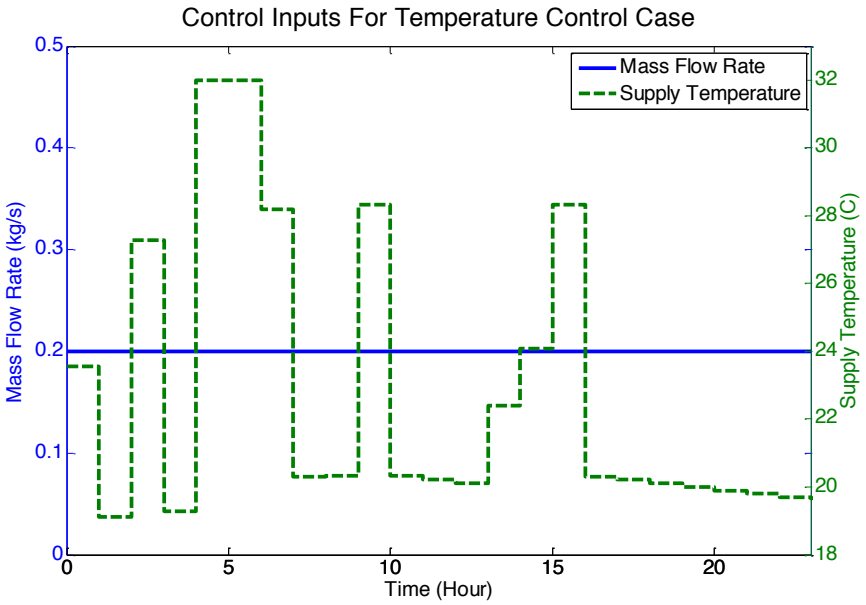

Figure 3.5: Control inputs for supply temperature control case.

3.3 Price Minimization with Mass Flow Rate Control

The system was next simulated in the mass flow rate control mode. The supply air temperature of the HVAC system was set to a constant value and the heat supplied to the room was varied through varying the supply temperature of the heat pump.

As with the previous supply temperature control results, the system was tuned to chose the optimal set point. The tuning curve for the constant supply temperature set point is shown in Figure 3.6.

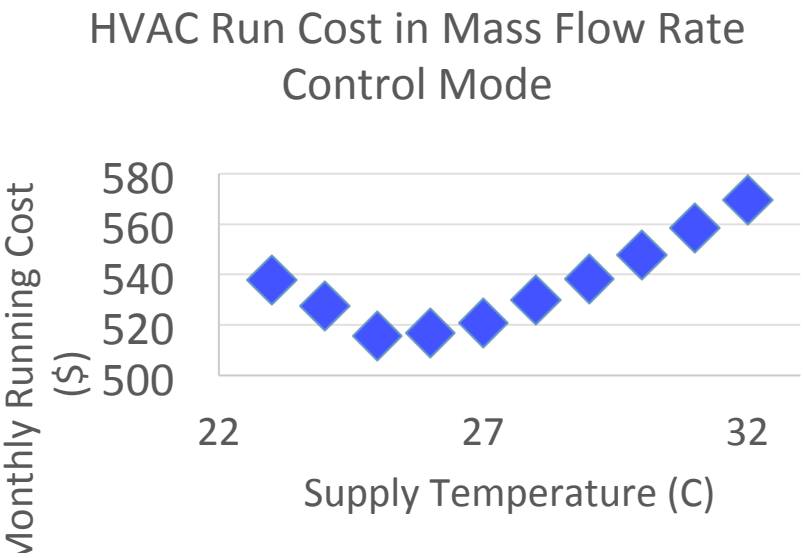

Figure 3.6: Tuning Curve for Mass Flow Rate Control. The price is minimized for this mode when supply air temperature is set to 25 C.

The optimal set point for the temperature was found to be 25 C. The monthly cost to run the HVAC system increases if the supply temperature is increased or decreased.

The results of an optimal control simulation over 24 hours with this supply temperature is shown in Figure 3.7. Some preheating occurs when prices are lower so that the actuation can be low during hours with higher prices. In general the room temperature stays close to the lower limit.

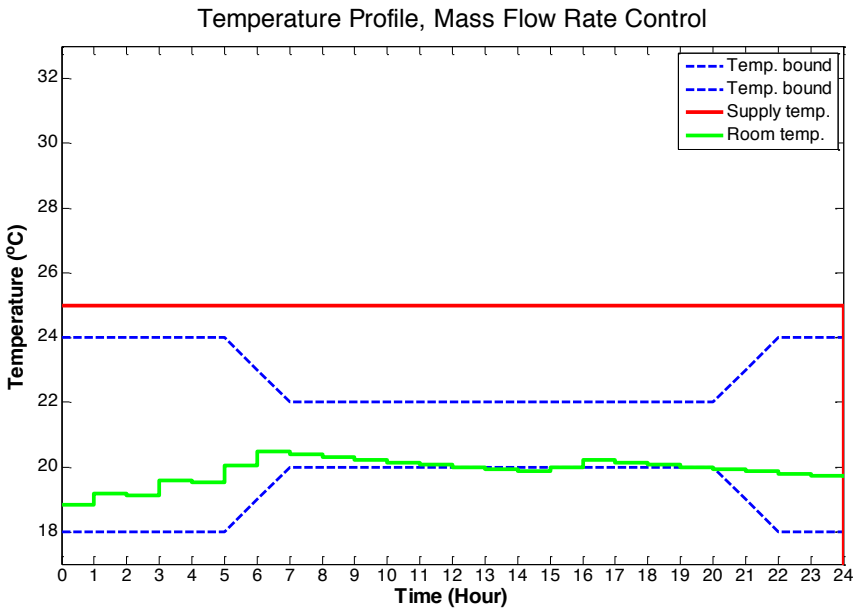

Figure 3.7: Temperature profile for mass flow rate control case.

The control inputs for the HVAC system are shown in Figure 3.8. The supply temperature is set to 25 C as chosen by the tuning process. The mass flow rate updates every hour as chosen by the optimal control algorithm.

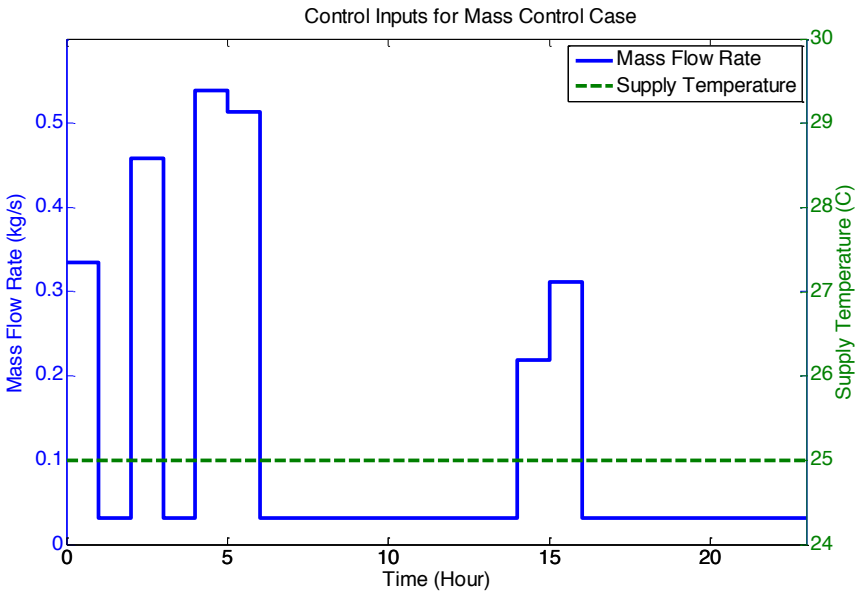

Figure 3.8: Control inputs for mass flow rate control case. The constant supply temperature value was determined by a tuning process. The mass flow rate values are determined in real time by the optimal control algorithm.

3.4 Price Minimization with Combined Mass Flow Rate and Supply Temperature Control ('Nonlinear' Case)

With solutions found for the cases with separate mass flow rate and supply temperature control, the combined case will now be solved. In this case, both supply temperature and mass flow rate of the HVAC system can be updated every hour. This has the effect of strengthening the actuators; there is more flexibility in the amount of heat transfer in any hour, giving the potential for a more optimal set of inputs. This problem also has added computational complexity compared to the two previous cases. As previously explained in Section 2., the dynamics of this control problem are nonlinear when both mass flow rate and supply air temperature are variable. This additional computational complexity makes the problem more difficult to formulate and solve, contrasting the previous linear simulations to this nonlinear simulation. For convenience the combined mass flow rate and supply temperature problem formulation will henceforth be referred to as the nonlinear case.

Figure 3.9 shows the resulting temperature profile from the combined mass flow rate and supply temperature control case. The advantage of this control mode can be seen in the supply air temperature profile. The number of hours where the HVAC is strongly actuated is decreased compared to the solo supply temperature case.

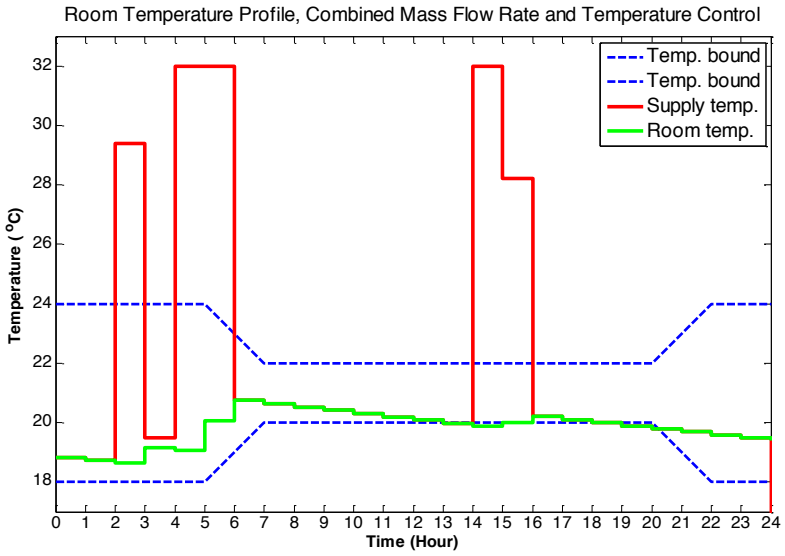

Figure 3.9: Temperature profile for combined supply temperature and mass flow rate control.

The control inputs shown in Figure 3.10 show the advantage of the combined control case. At times when power is cheap, both the mass flow rate and supply temperature increase. Otherwise, both inputs are set to their minimum. These plots clearly illustrate that the nonlinear case has the effect of making the actuator stronger.

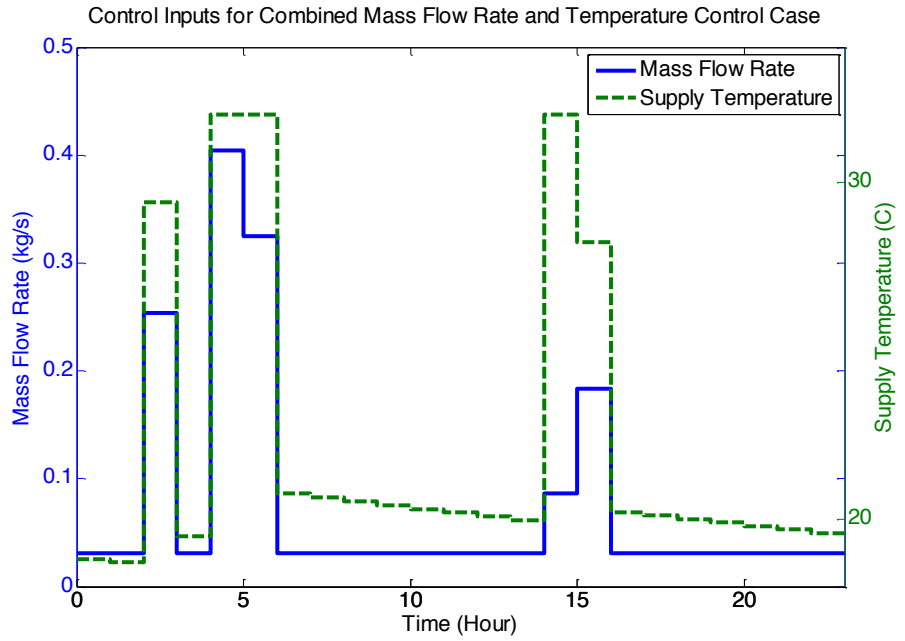

Figure 3.10: Control inputs for combined supply temperature and mass flow rate control case.

The behavior of the combined control case is also illustrated in Figures 3.11 and 3.12. They show the dynamic price profile used during the simulation, and the HVAC power consumption and run cost at each hour. The strong actuator provided by the combined control means that power spikes only occur during hours with low price.

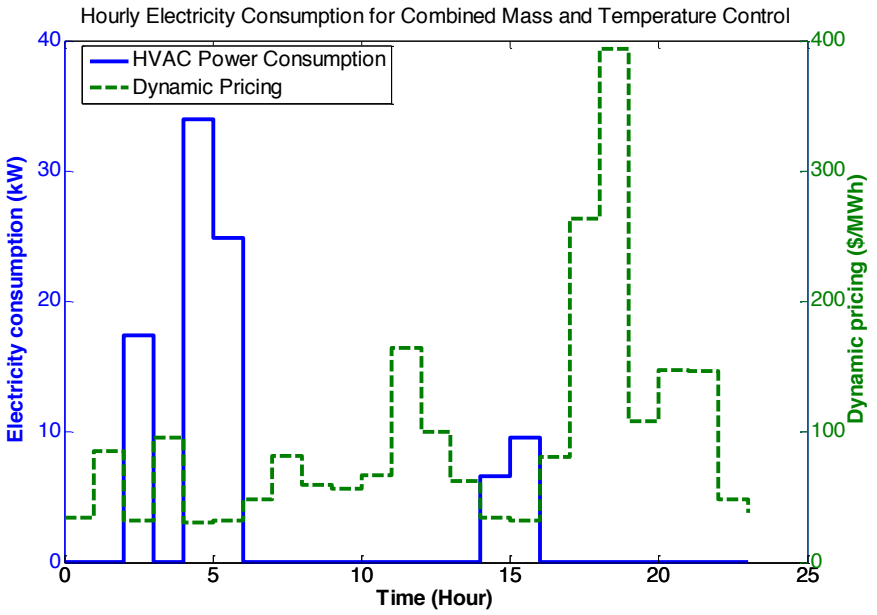

Figure 3.11: Hourly Power Consumption for nonlinear case.

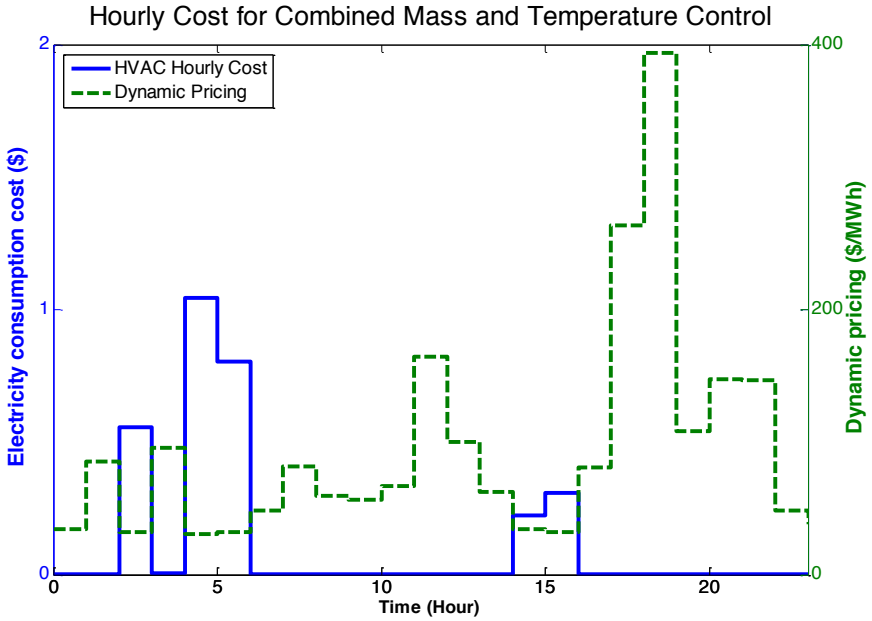

Figure 3.12: Hourly Cost for nonlinear case.

3.5 Control Mode Comparison

A comparison of the above results is shown in Table 3.1 below.

Table 3.1: Comparison of cost and electricity consumption for all four control modes

Control Mode	**Mass Flow Rate (kg/s)**	**Supply Temperature (C)**	**Monthly Cost**	**Daily Electricity Consumption**	**Cost Saving (%)**	**Energy Saving (%)**
RBC	.2 (.4)	32	$850	326 kWh	-	-
Mass Control	Variable	25	$516	242 kWh	39%	25%
Temperature Control	.2	Variable	$420	219 kWh	50%	33%
Nonlinear	Variable	Variable	$410	210 kWh	52%	36%

The solo mass flow rate control, solo temperature control, and combined mass flow rate and temperature control are compared to the results of a typical Rule Based Controller (RBC).

All three MPC control cases show savings compared to the RBC. The combined mass flow rate and temperature control case shows the best savings, as expected. Having two design variables, which equates to a stronger actuator for the HVAC system in this case, allows for more cost savings.

The mass control case is considerably more expensive than the temperature control case. This is because some air must always flow into the zone to meet ventilation requirements. So, even during hours when power is expensive, some air must be heated to the chosen set point. In the temperature control case, the supply temperature can be set equal to the room temperature during hours where power is expensive, and air recirculates without heating, which minimizes this problem. The

combined case has this same advantage, plus the ability to more strongly actuate by increasing both mass flow rate and supply temperature during times with cheap power.

A detailed comparison of the three MPC cases is shown in Figures 3.13 and 3.14. These plots compare the hourly power consumption of each case. We once again clearly see where the advantage of combined mass flow rate and supply temperature control comes from, and the disadvantage of mass flow rate control. Mass flow rate control and temperature control must run the HVAC more during hours when price is relatively high. The combined control case can restrict actuation to hours with relatively price and still remain in temperature bounds, since the HVAC system is able to actuate more strongly during those hours.

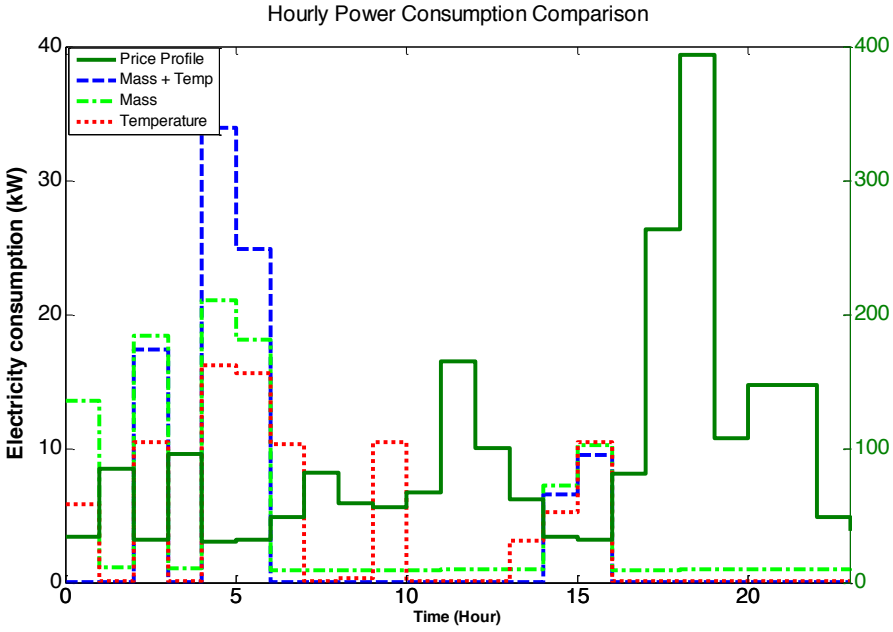

Figure 3.13: Comparison of hourly power consumptions.

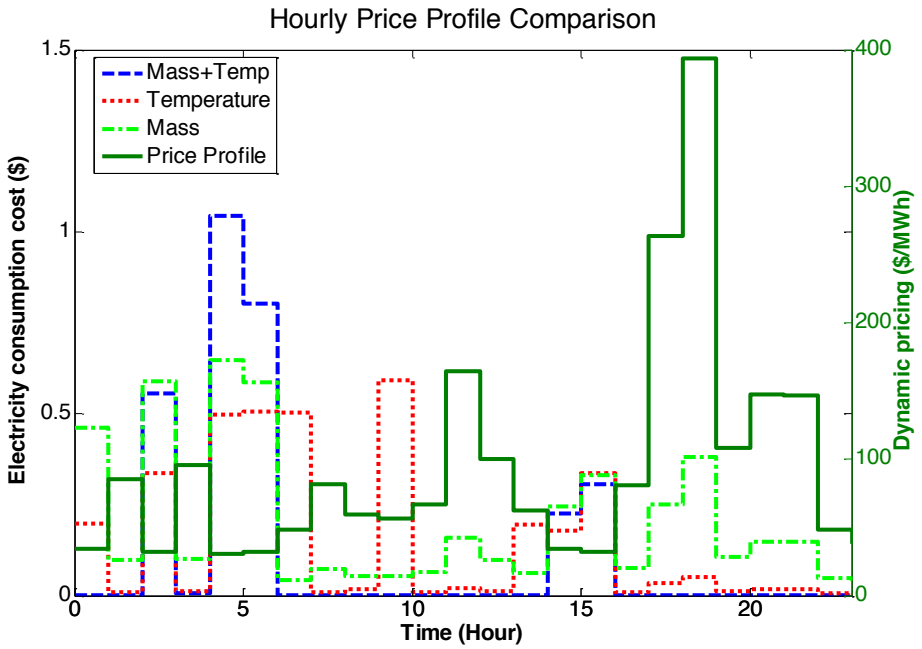

Figure 3.14: Comparison of hourly run cost.

The previous results show that there is a clear advantage to utilizing optimal control for the building's HVAC system. All three optimal control cases show substantial savings compared to the rule based control case.

3.6 Price Optimization with Battery Energy Storage

In the preceding results, the cost of running the HVAC system was decreased by using an optimal control algorithm. The hardware used in the energy management system was not changed from the base RBC case. The next step is to further increase the system's performance by adding an energy storage system to the building.

Adding Energy Storage Systems (ESS) can increase the performance of smart buildings. ESS can store energy from renewable energy sources for later use. They can also be used to store power from the grid during hours with low price or low demand, and then used to power the building during later hours when drawing power from the grid would be more expensive.

Energy storage has been utilized in previous MPC studies. This study will incorporate battery energy storage with the combined control of the HVAC's mass flow rate and supply temperature.

A model was developed to simulate the system with the addition of a battery. The model for the LG Chem battery was previously developed and presented in Chapter 2. The map for this battery's maximum charge and discharge power was available in the battery manual [26]. Using this model, the new optimization problem is:

$$\min_{I_e,\overline{\epsilon}\underline{\epsilon}}\{(I_e \cdot P_{Dyn}^T) + \rho(|\overline{\epsilon}_t|_1 + \left|\underline{\epsilon_t}\right|_1)\} \tag{3.12}$$

subject to:

$$x_{t+k+1|t} = A\, x_{t+k|t} + Bu_{t+k|t} + Ed_{t+k|t} \tag{3.13}$$

$$y_{t+k|t} = C\, x_{t+k|t} \tag{3.14}$$

$$SOC_{t+k+1|t} = SOC_{t+k|t} + \frac{P_{charge} - P_{discharge}}{V\, C_B} \tag{3.15}$$

$$\underline{\mathcal{U}} \leq u_{t+k|t} \leq \overline{\mathcal{U}} \tag{3.16}$$

$$\underline{\delta\mathcal{U}} \leq u_{t+k+1|t} - u_{t+k|t} \leq \overline{\delta\mathcal{U}} \tag{3.17}$$

$$\underline{T}_{t+k|t} - \underline{\mathcal{E}}_{t+k|t} \leq y_{t+k|t} \leq \overline{T}_{t+k|t} + \overline{\mathcal{E}}_{t+k|t} \tag{3.18}$$

$$0 \leq P_{charge_{t+k|t}} \leq P_{MAXcharge_{t+k|t}} \tag{3.19}$$

$$0 \leq P_{discharge_{t+k|t}} \leq P_{MAXdischarge_{t+k|t}} \tag{3.20}$$

$$0 \leq P_{discharge_{t+k|t}} \leq VC_i \tag{3.21}$$

$$\underline{\mathcal{E}}_{t+k|t}, \overline{\mathcal{E}}_{t+k|t} \geq 0 \tag{3.22}$$

Here, SOC is the state of charge of the battery, P_{charge} is the power to charge the battery, $P_{discharge}$ is the power discharged from the battery, V is the voltage across the battery, C_B is the capacity of the battery. $P_{MAXcharge}$ is the upper limit on power to charge the battery and $P_{MAXdischarge}$ is the upper limit on the discharge power of the battery. C_i is the current of the battery. The remaining symbols share definitions with the problem formulation from Equations 3.1 to 3.11.

Where the objective function is defined using a new Energy Index:

$$I_e = \sum_{t=0}^{24} \left[P_h(t) + P_c(t) + P_f(t) + P_{charge}(t) - P_{discharge}(t) \right] \tag{3.23}$$

Where

$$P_h(t) = \dot{m}_i^r(t) c_{p,air} \left[T_h(t) - T_{r_i}(t) \right] \tag{3.24}$$

$$P_c(t) = \dot{m}_i^r(t) c_{p,air} [T_{r_i}(t) - T_c(t)] \tag{3.25}$$

$$P_f(t) = \gamma (\dot{m}_i^r)^3 \tag{3.26}$$

The system was simulated with the addition of the battery. Combined mass flow rate and supply temperature control was chosen since it gave the best performance out of the preceding results.

The room temperature profile is shown in Figure 3.15. The room temperature stays within the specified comfort constraints over the 24 hour period shown. There is less preheating when compared to the simulations without battery storage.

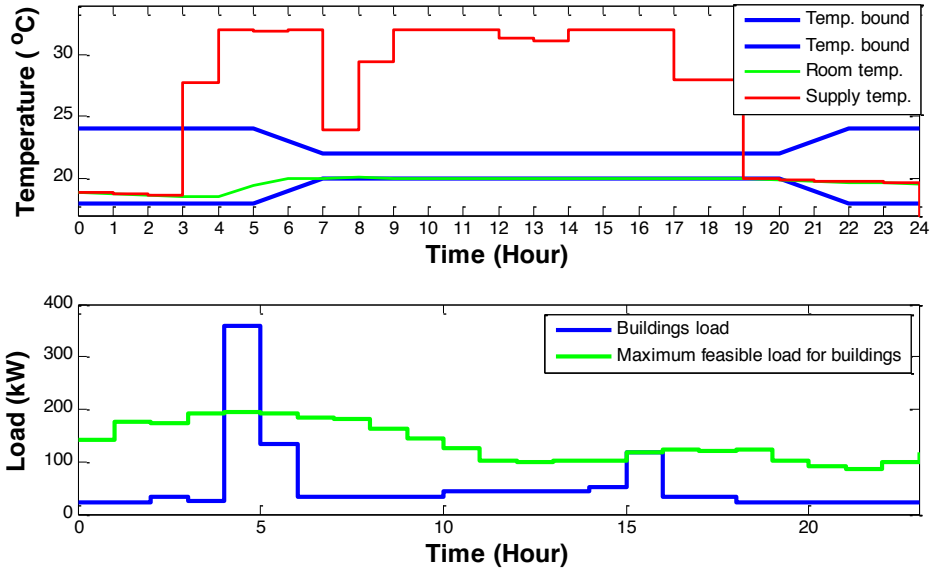

Figure 3.15: Room Temperature profile for ESS simulation

Figure 3.16 shows the net energy flow per hour between the grid, HVAC system, and battery. This figure illustrates how the battery benefits the system performance. The battery is charged at an hour early in the morning when the price is low. At the same time, the HVAC system is strongly actuated to preheat the building. Then, the battery is used during the day to power the HVAC system, and maintain comfort in the room, without drawing large amounts of power from the grid. The battery is then charged in the late afternoon when it meets its minimum SOC value. Negative energy values in Figure 3.16 represent energy discharging from the battery to power the HVAC system.

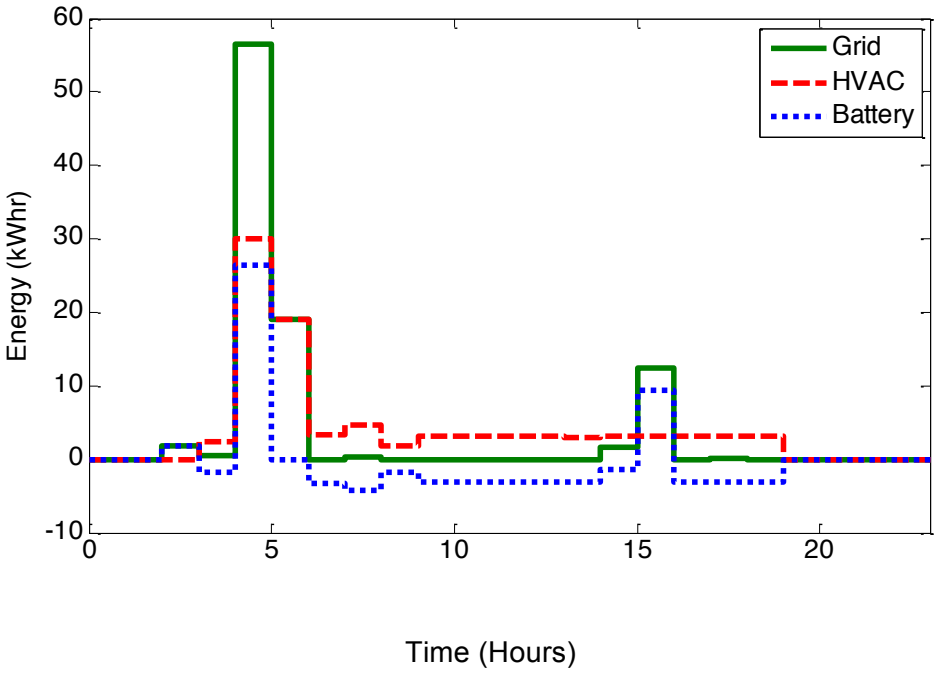

Figure 3.16: System energy flow

Figure 3.17 illustrates that the demand on the grid for power is concentrated on the hours where the price of power is low. The same concentration in power consumption was present in the system without the battery. The difference is that some of the power is used to charge the battery instead of directly heating the room. The power is then used at a later time by the HVAC system. This reduces the amount of preheating by the system, which means less energy is wasted heating the room more than necessary. This allows for savings in both cost and energy consumption.

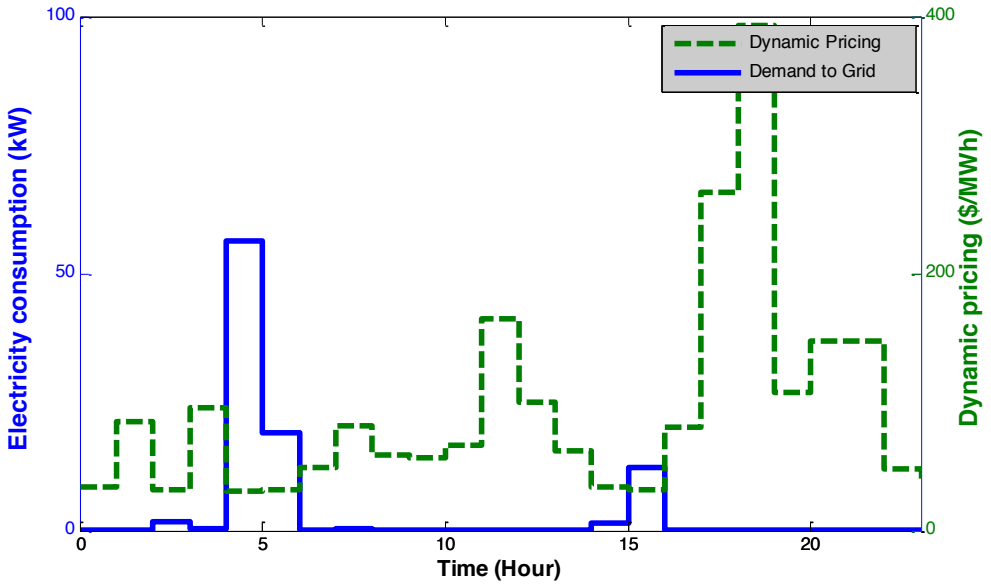

Figure 3.17: Hourly Electricity Consumption with Battery ESS

The battery's state of charge (SOC) is shown in Figure 3.18. When the battery is charged early in the day, the SOC increases to its upper limit. The battery then is used over the next several hours to power the HVAC system, and the SOC decreases. The trend in SOC clearly aligns with the power flow of the battery.

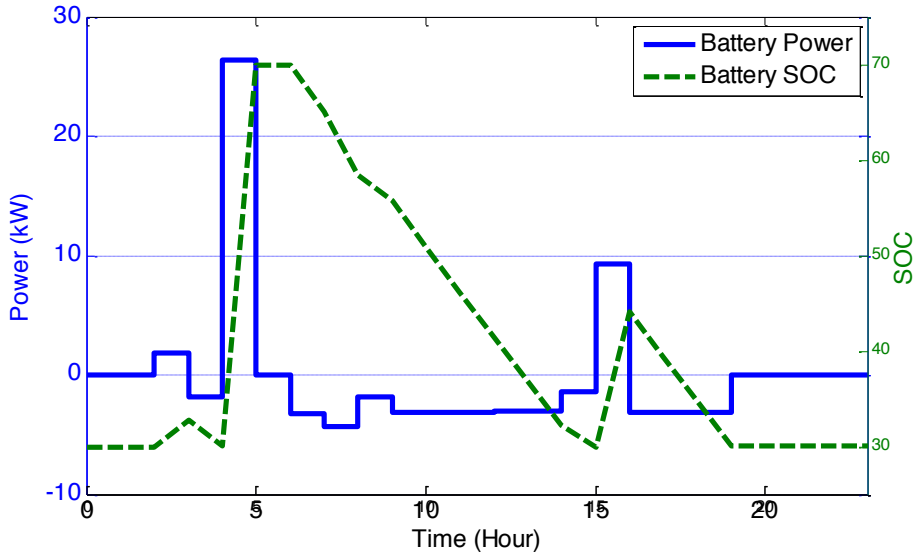

Figure 3.18: Battery SOC over the day

The cost and energy consumption results are shown in Table 3.2.

Table 3.2: Results of Price optimization with Battery Energy Storage, compared to the RBC results, and MPC with the battery storage system.

Control Mode	**Monthly Cost**	**Daily Electricity Consumption**	**Cost Saving (%)**	**Energy Saving (%)**
RBC	$850	326 kWh	-	-
Price Control with ESS	$405	209 kWh	52.3%	35.8%
Price Control	$410	210 kWh	51.7%	35.6%

The results show that the battery storage system is able to reduce the monthly cost of running the HVAC system, while increasing the energy efficiency. However, the performance increase from energy storage is small compared to the effect of using optimal control. These results would show that the control algorithm has a much larger impact on the system performance than adding an energy storage system. The type of battery being used in the model may be impacting this result, and a battery designed explicitly for use in building energy storage could have properties which would show better performance.

3.7 Comparison Using Energy Cost Function

A special case of the previous results will be considered. In cases where the price of electricity is static instead of dynamic, the problem reduces to optimizing the energy consumption. In this case the cost is set to a constant value over the optimization domain.

The optimization problem can be stated as:

$$\min_{I_e,\overline{\epsilon}\underline{\epsilon}}\{(I_e) + \rho(|\overline{\epsilon}_t|_1 + \left|\underline{\epsilon_t}\right|_1)\} \tag{3.27}$$

subject to:

$$x_{t+k+1|t} = A\, x_{t+k|t} + Bu_{t+k|t} + Ed_{t+k|t} \tag{3.28}$$

$$y_{t+k|t} = C\, x_{t+k|t} \tag{3.29}$$

$$\underline{\mathcal{U}} \;\; \leq u_{t+k|t} \leq \overline{\mathcal{U}} \tag{3.30}$$

$$\underline{\delta\mathcal{U}} \leq u_{t+k+1|t} - u_{t+k|t} \leq \overline{\delta\mathcal{U}} \tag{3.31}$$

$$\underline{T}_{t+k|t} - \underline{\mathcal{E}}_{t+k|t} \leq y_{t+k|t} \leq \overline{T}_{t+k|t} + \overline{\mathcal{E}}_{t+k|t} \tag{3.32}$$

$$\underline{\mathcal{E}}_{t+k|t}, \overline{\mathcal{E}}_{t+k|t} \geq 0 \tag{3.33}$$

The objective function is defined using the Energy Index (I_e):

$$I_e = \sum_{t=0}^{24}\left[P_h(t) + P_c(t) + P_f(t)\right] \tag{3.34}$$

Where

$$P_h(t) = \dot{m}_i^r(t)c_{p,air}\left[T_h(t) - T_{r_i}(t)\right] \tag{3.35}$$

$$P_c(t) = \dot{m}_i^r(t)c_{p,air}[T_{r_i}(t) - T_c(t)] \tag{3.36}$$

$$P_f(t) = \gamma(\dot{m}_i^r)^3 \tag{3.37}$$

Note that the term for dynamic pricing is now absent from the optimization problem. All symbols retain their defintions from Equations 3.1-3.11.

The system was simulated for energy optimization using supply temperature control, mass flow rate control, and combined supply temperature and mass flow rate control. Figure 3.19 shows a comparison of the daily energy consumption of each simulation.

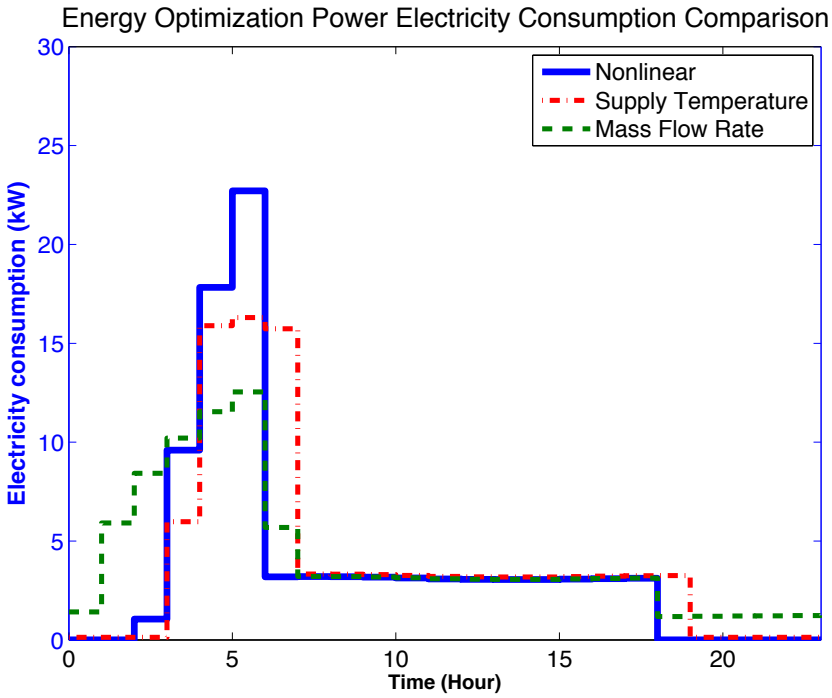

Figure 3.19: Energy optimization comparison

The combined mass flow rate and supply temperature control case has the strongest maximum actuation and has the highest peak hourly energy use. The effect of these different control modes is compared in Table 3.3.

Table 3.3: Comparison of Control Modes for Energy Optimization

Control Mode	**Mass Flow Rate (kg/s)**	**Supply Temperature (C)**	**Daily Electricity Consumption**	**Energy Saving (%)**
RBC	0.2	Variable	326 kWh	-
Mass Control	Variable	25	225 kWh	31%
Temperature Control	0.2	Variable	200 kWh	39%
Mass and Temperature Control (Nonlinear Case)	Variable	Variable	194 kWh	40.4%

The results show that the combined mass flow rate and supply temperature control case has the best performance. As in the price minimization case, the additional control variable leads to higher relative performance. Mass control has the worst performance of the three optimal control formulations. This is again due to the minimum mass flow rate required to meet ventilation requirements.

A comparison of the price results shown in Table 3.1 and 3.3 highlights the scenario where of combined mass flow rate and supply temperature control has the greatest advantage. Under dynamic pricing, the nonlinear case has a 2% price advantage over the linear supply temperature control problem. In energy optimization with flat pricing, the price advantage (which is equivalent with the energy advantage under flat pricing) is 1.4%. The nonlinear problem has a greater advantage under dynamic pricing. The additional strength of the actuator yields better results in both scenarios, but the nonlinear controller shows more promise in a dynamic pricing environment.

Chapter 4

4 Building to Grid Optimization

4.1 Limitations of Building-level Control

The control algorithm proposed in Chapter 3 was able to successfully decrease the cost of running the building's HVAC system through MPC. But, cost is not the only consideration when designing a smart grid. In Figure 4.1, the building load profile for the building under price control is shown. This load profile includes the required HVAC load, and the base building load from lighting and appliances. Also shown is an example of a possible maximum load which can be provided by the electric grid. For more information on how the maximum load profile is calculated, refer to [16].

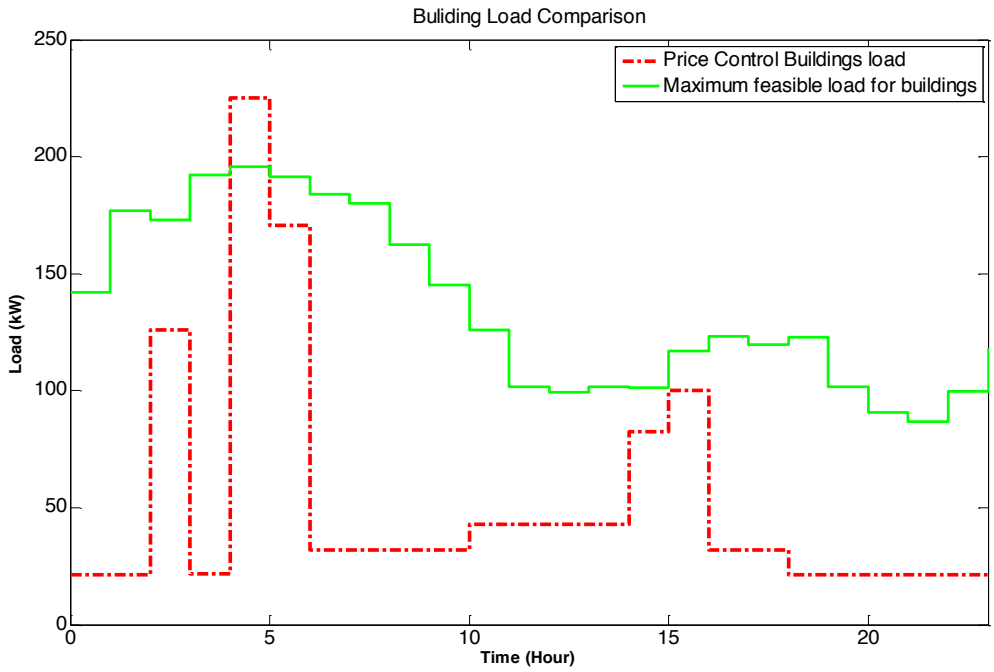

Figure 4.1: Price control load profile. The maximum feasible power load is violated.

In this case, the load violates the maximum allowable load. Since the objective function does not consider the size of the peak load in any way, this is not surprising. This issue will be motivation to develop a new control algorithm which considers the effect of the grid.

4.2 Grid Integration

Balancing the power load is an important goal for the power distribution grid operator. Successful load balance and regulation have a variety of factors. Power provided by renewable energy sources (wind, PV panels) is variable and increases the complication of the system. Large peak loads can require extra infrastructure in order to fully provide the demanded load. In order to maintain a balanced load, it is beneficial to employ load balancing and curtailment strategies.

In the previous chapter's results, the objective was focused on providing savings for the consumer in the power grid. For example, the objective under price control was to maintain temperature comfort constraints while minimizing cost to the consumer. This benefits the individual consumer, but does not necessarily benefit the power supplier or the performance of the power grid as a whole.

To study the optimization effects on the grid, a model for building to grid (B2G) interaction must be considered. The power grid is modeled as a connected system of nodes. Buildings can be connected at any node and draw a load from the grid. This system is illustrated in Figure 4.2.

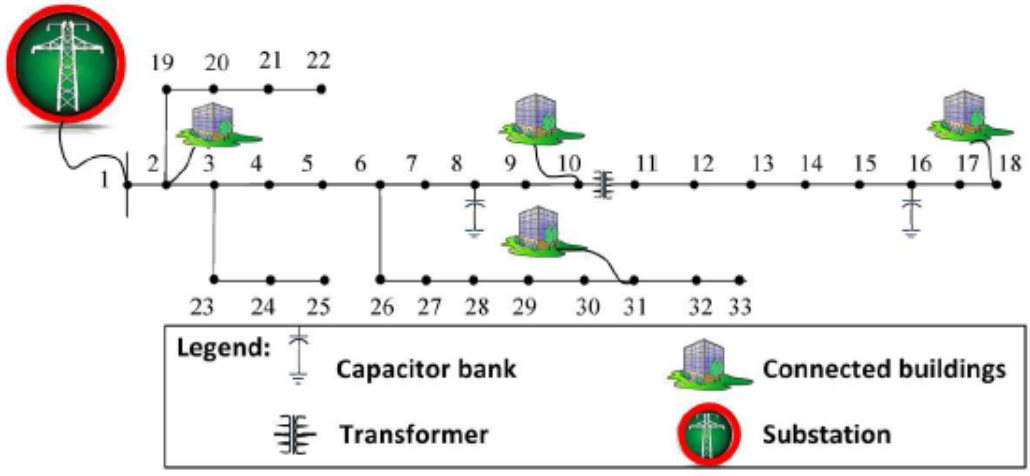

Figure 4.2: Grid Model[15]. © 2015 IEEE.

Another approach is to focus optimization on the performance of the grid as a whole. The power supplier benefits if the grid load is relatively flat over time. High demand at peak times requires more infrastructure, which is wasted at off-peak times. Ideally, demand would be constant, and allow for optimal use of all power generation sources at all times.

4.3 Load Factor Optimization

In order to achieve this goal, the concept of the load factor will be introduced into the optimization. Load factor is defined as

$$LF = \frac{P_{avg}}{P_{\infty}} \tag{4.1}$$

Where P_{∞} is maximum power is load and P_{avg} is the average power load. In the problem formulation, load factor can be maximized by minimizing the infinity norm of the building load. To maximize load factor, the MPC problem can be formulated as:

$$\min \ \{\beta/LF + \rho(|\overline{\epsilon}_t|_1 + \left|\underline{\epsilon_t}\right|_1\} \tag{4.2}$$

subject to:

$$x_{t+k+1|t} = A\, x_{t+k|t} + Bu_{t+k|t} + Ed_{t+k|t} \tag{4.3}$$

$$y_{t+k|t} = C\, x_{t+k|t} \tag{4.4}$$

$$\underline{\mathcal{U}}_{t+k|t} \leq u_{t+k|t} \leq \overline{\mathcal{U}} \tag{4.5}$$

$$\underline{\delta\mathcal{U}} \leq u_{t+k+1|t} - u_{t+k|t} \leq \overline{\delta\mathcal{U}} \tag{4.6}$$

$$\underline{T}_{t+k|t} - \underline{\mathcal{E}}_{t+k|t} \leq y_{t+k|t} \leq \overline{T}_{t+k|t} + \overline{\mathcal{E}}_{t+k|t} \tag{4.7}$$

$$\underline{\mathcal{E}}_{t+k|t}, \overline{\mathcal{E}}_{t+k|t} \geq 0 \tag{4.8}$$

Here β is the weight on the load factor in the objective function and LF is the load factor. The remaining symbols retain their defintions from Section 3.1.

Note that price is not considered in this objective function. The objective function now only has terms dependent on the infinity norm on the power consumption, and a penalty for violation of the room temperature soft constraints.

Figure 4.3 shows the room temperature profile for a simulation using the load factor optimization algorithim. The overall bulding load is relatively constant compared to the previous price and energy optimization simulations.

Load and Temperature Profiles for Load Factor Objective Function

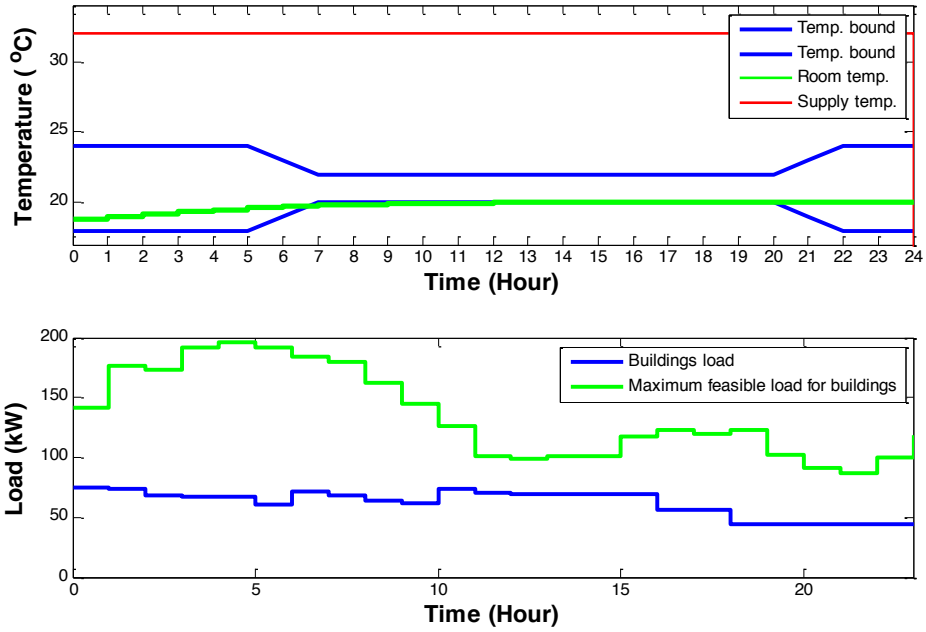

Figure 4.3: Temperature profile and load profile for Load Factor Control

As expected, the building load profile is very steady when load factor optimization is employed. The temperature raises to the daytime minimum and is maintained there to maintain a constant load. In Figure 4.4, the electricity consumption used under load factor control is shown.

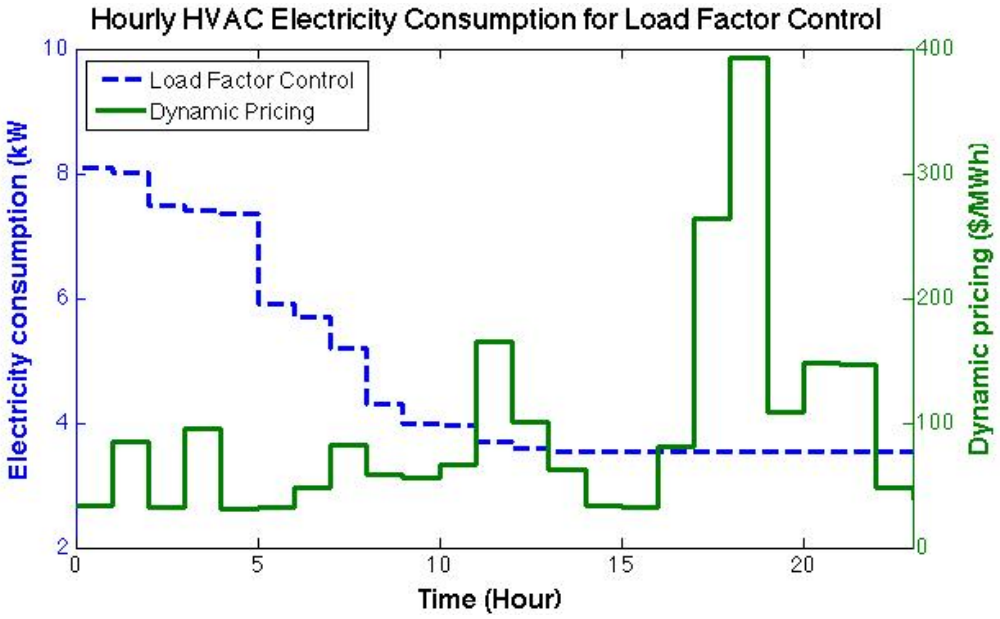

Figure 4.4: Electricity Consumption Profile for Load Factor Control

We can see from the electricity consumption that the consumed power is higher in the morning to reach the daytime minimum temperature, in order to maintain the comfort constraints. Once this temperature is reached, the load stays constant.

In Figure 4.5, the load profile for price and load factor optimization are compared. The advantage provided to the grid distributor is clear; the balanced load is easier for the grid to manage and provide. By using the load factor objective function, the nodal load factor of the node being controlled is improved to .85. This results in a 130% improvement over the nodal load factor of .37 resulting from the price control results.

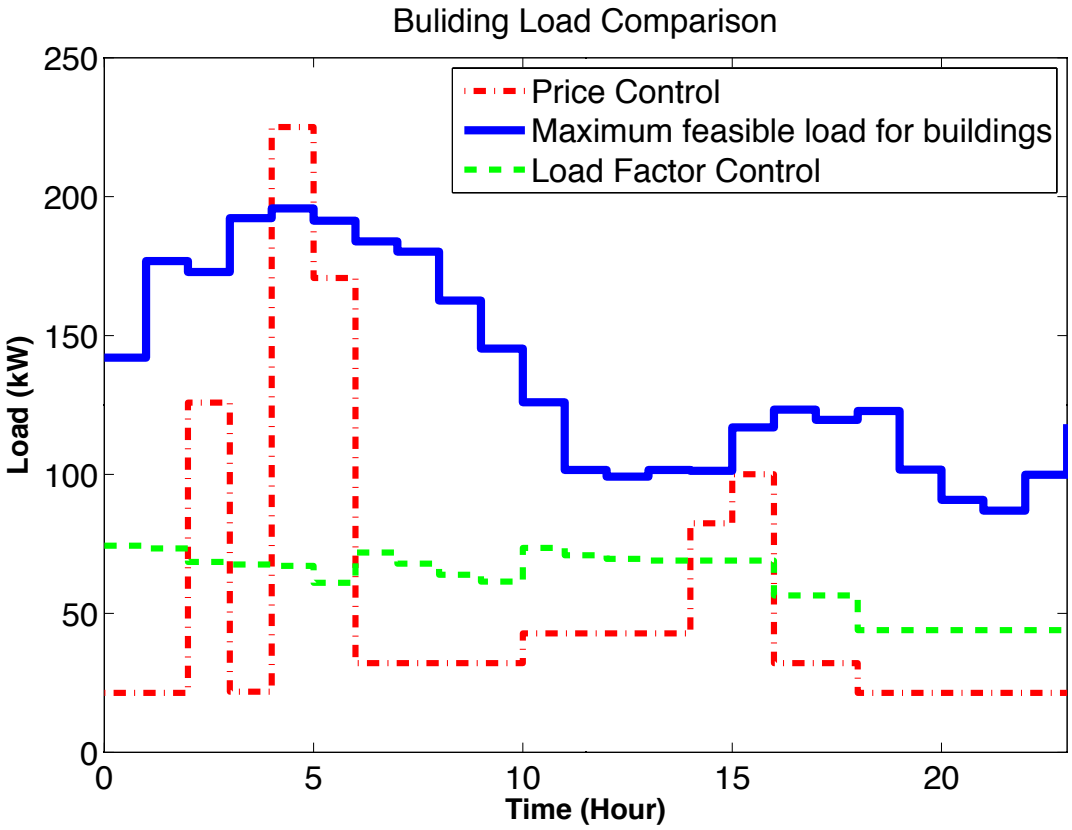

Figure 4.5: Comparison of load profiles between price control and load factor control

In Figure 4.6 there is a comparison of the hourly price of running the HVAC systems for the cases with price and load factor as the objective function. This illustrates the advantage provided by the price control objective function. By using load factor control, the monthly cost of running the HVAC system increases from $410 to $725.

The comparison of results between Load Factor and Price optimization is shown in Table 4.1 below.

Table 4.1: Comparison of Load Factor and Price Optimization Objective Functions

Objective Function	**Monthly Cost**	**Node Load Factor**
Load Factor	$725	..85
Price	$410	.37

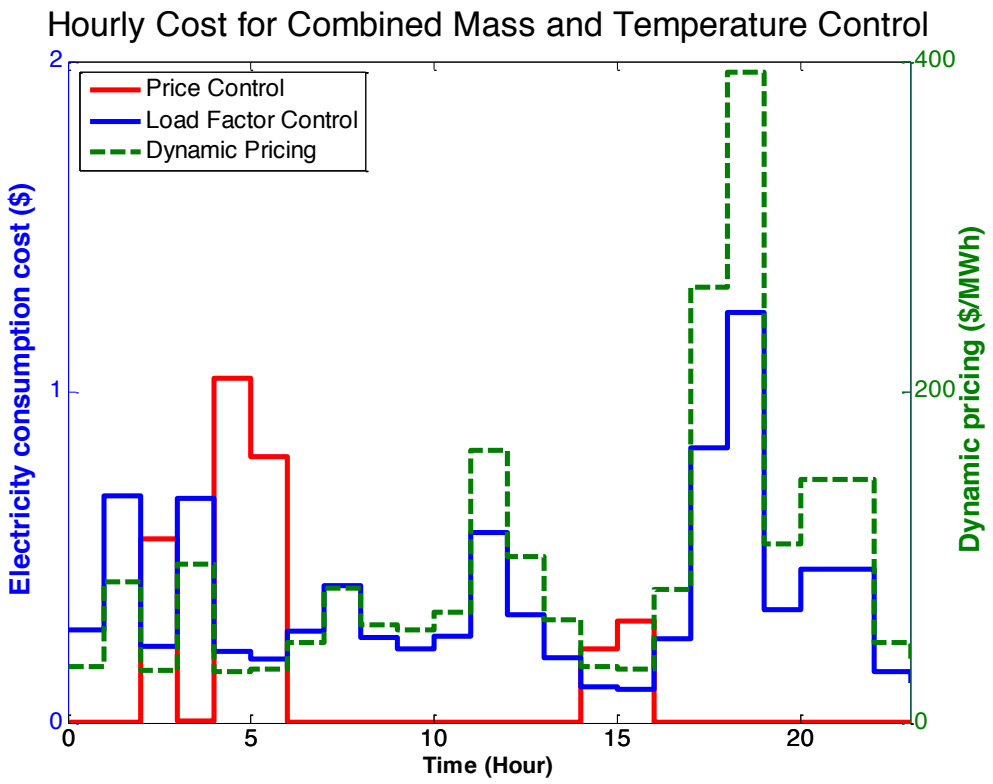

Figure 4.6: Comparison of price profiles between price control and load factor control

Under price control the system only actuates during hours with low price. The load factor controller maintains a constant load regardless of price, which has a large impact on price during peak hours where the dynamic pricing is high.

4.4 Building to Grid Integration

The previous results illustrate the tradeoff between load factor and price optimization for the smart grid. Maximizing the load factor benefits the distributor, but has a negative impact of the price for the consumer. In order to find a solution which benefits both the consumer and grid supplier, another approach can be taken which strikes a balance between maximizing the load factor and minimizing HVAC run cost. The objective function can directly consider both price and load factor, with weights on each. The MPC problem in this case is:

$$\min_{I_e,\overline{\epsilon}\underline{\epsilon}}\{\alpha(I_e \cdot P_{Dyn}^T) + \beta/LF + \rho(|\overline{\epsilon}_t|_1 + \left|\underline{\epsilon_t}\right|_1)\} \tag{4.9}$$

subject to:

$$x_{t+k+1|t} = A\, x_{t+k|t} + Bu_{t+k|t} + Ed_{t+k|t} \tag{4.10}$$

$$y_{t+k|t} = C\, x_{t+k|t} \tag{4.11}$$

$$\underline{U}_{t+k|t} \leq u_{t+k|t} \leq \overline{U} \tag{4.12}$$

$$\underline{\delta U} \leq u_{t+k+1|t} - u_{t+k|t} \leq \overline{\delta U} \tag{4.13}$$

$$\underline{T}_{t+k|t} - \underline{\mathcal{E}}_{t+k|t} \leq y_{t+k|t} \leq \overline{T}_{t+k|t} + \overline{\mathcal{E}}_{t+k|t} \tag{4.14}$$

$$\underline{\mathcal{E}}_{t+k|t}, \overline{\mathcal{E}}_{t+k|t} \geq 0 \tag{4.15}$$

Here α is the weight on the monatary run cost of the HVAC system. The remaining symbols retain their definitions from the load factor control formulation in 4.1-4.8.

By varying the weights in the objective function, the system can be tuned to more strongly consider either price or load factor. This tuning process was performed by varying the α and β values over a chosen range. The range of values was chosen such that the system would maintain a comfortable in-room temperature during the optimization. Figure 4.7 shows the HVAC run cost surface over this tuning range.

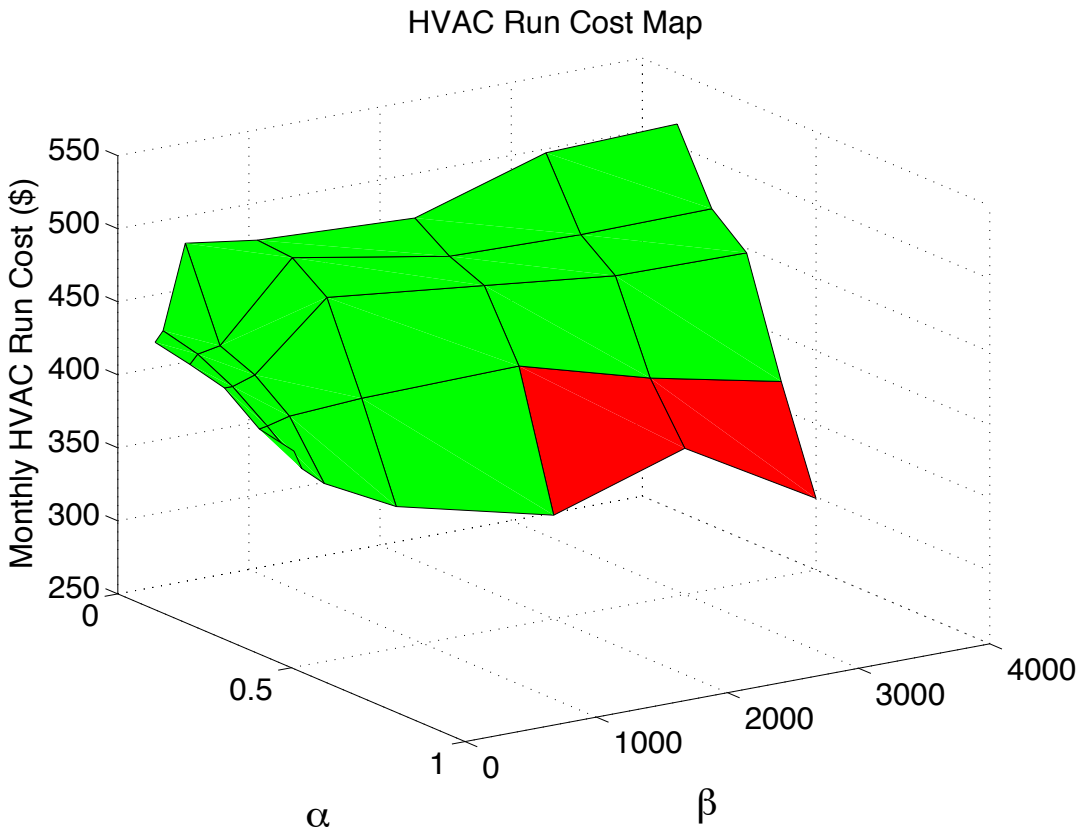

Figure 4.7: Surface of HVAC Run cost over tuning space of objective function weights. Points colored red violated the room comfort constraints and were not considered as viable solutions.

Increasing the α value in the objective function decreases the run cost, as expected. The red region in Figure 4.7 are points where the comfort constraints were not met. If price is of higher priority than load factor, this map can be used to choose appropriate tuning parameters.

Figure 4.8 shows the load factor surface over this tuning range.

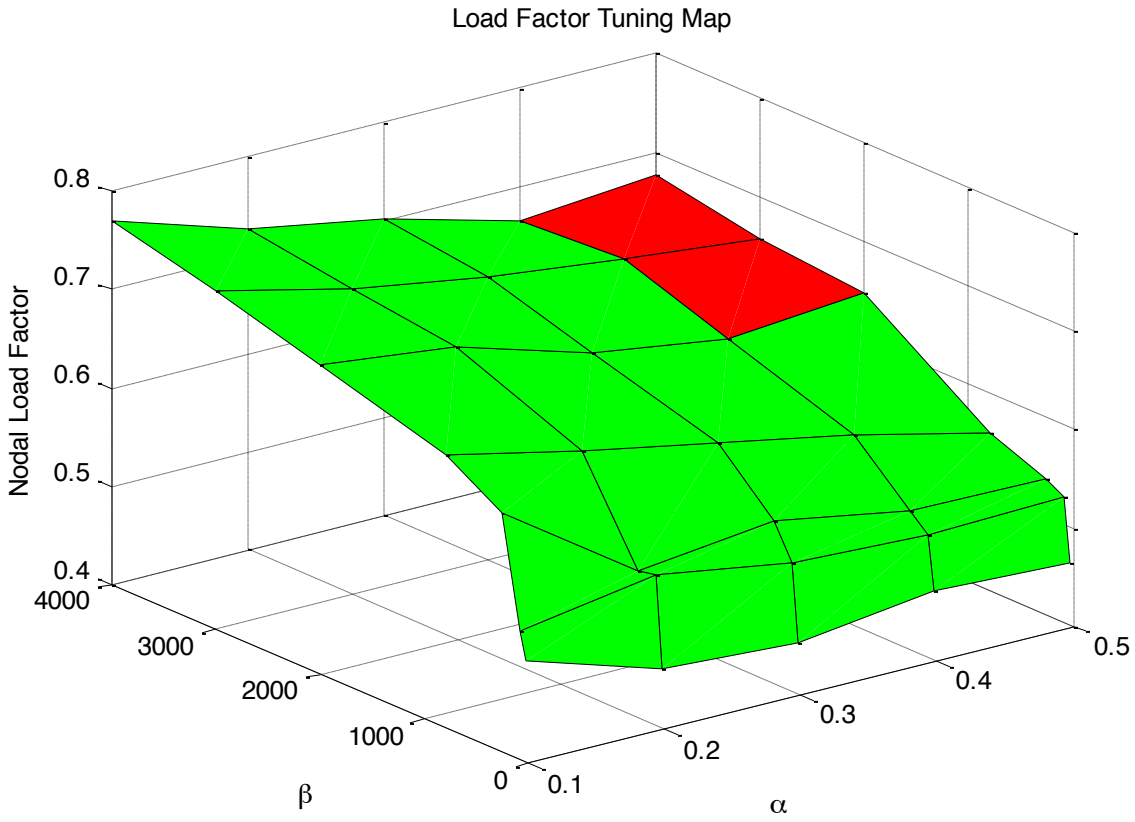

Figure 4.8: Surface of load factor values over space of objective function weights. Points colored red violated the room comfort constraints and were not considered as viable solutions.

Increasing the β value in the objective function increases the load factor, as expected. The red region in Figure 4.8 are points where the comfort constraints were not met. If load factor is the only objective, this map can be used to choose appropriate tuning parameters.

This tuning process can be used to find weights which give optimal performance. Some metric must be defined to form the basis for this comparison. We will define the comparative index I_{norm}:

$$I_{norm} = .5\ (1 - \frac{Pr}{\mathrm{Pr}_{existing}} + (LF_{Node})) \tag{4.16}$$

where Pr is the cost in dollars to run the HVAC system, $\mathrm{Pr}_{existing}$ is the cost to run the RBC controller, and $\mathrm{LF}_{\mathrm{Node}}$ is the nodal load factor. I_{norm} allows for a fair

comparison of the performance between points. The performance metric over the tuning space are shown below in Figure 4.9.

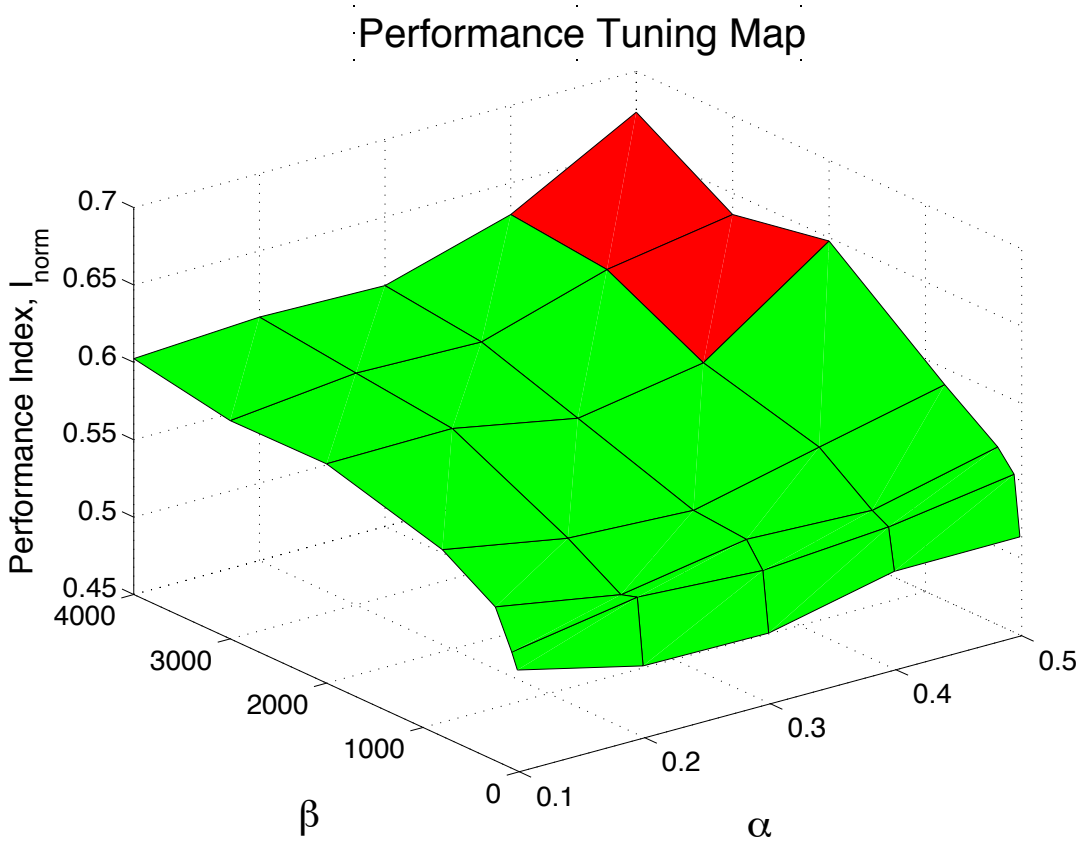

Figure 4.9: Surface of performance metric values over space of objective function weights

The system shows better performance when both α and β are increased. This is because the weight on the terms used to measure performance, price and load factor, are increasing compared to the weight assigned to the soft comfort constraints. The points shown in red are areas where the room temperature comfort constraints are not satisfied during the optimization. This occurs as the weights on performance increase compared to the constant weight on comfort. Excluding the points where comfort constraints were not met, the performance index was highest at the point:

$$(\alpha, \beta) = (0.3, 4000)$$

The performance of this control mode with these α and β settings can be compared to other control modes. Using this same tuning parameters, the controller was simulated with the three optimal control modes used in Chapter 3 and the results were compared. For solo mass flow rate and solo supply temperature control, the same settings were used as in Chapter 3. The results are shown below in Table 4.2.

Table 4.2: Comparison of B2G results

Control Mode	**Monthly Cost**	**Node Load Factor**	**Normalized Index**
Mass Control	$516	.59	.51
Temperature Control	$493	.74	.60
Mass + Temp	$457	.71	.61

Using the performance index as a metric, combined mass and temperature control has the best performance. This is expected, since the combined mass and temperature case has an extra control variable when compared to the other two simulations, and should at worst have equal results. The combined mass flow rate and temperature control results are shown in Figure 4.10.

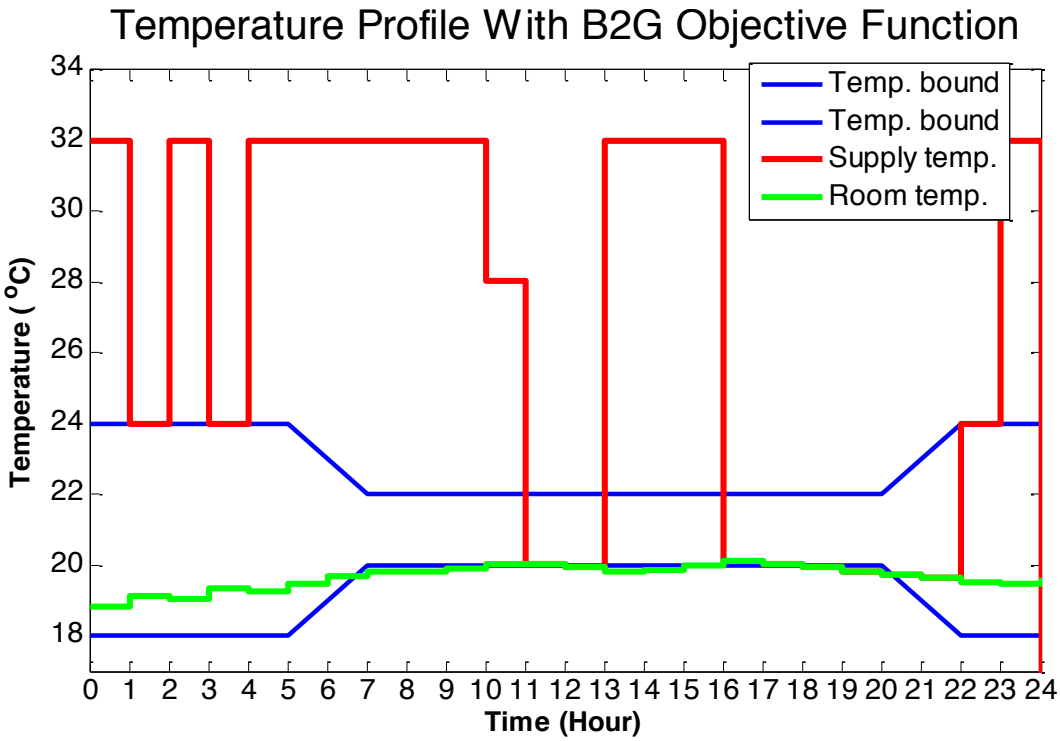

Figure 4.10: Temperature profile results from simulated using tuned B2G control. $(\alpha, \beta) = (0.3, 4000)$

The amount of hours with high actuation is large compared to the price objective function. The temperature profile does not always track the lower limit because the objective function is not only attempting to minimize price, but also maintain a constant load.

The load profile from the B2G control mode is shown in Figure 4.11.

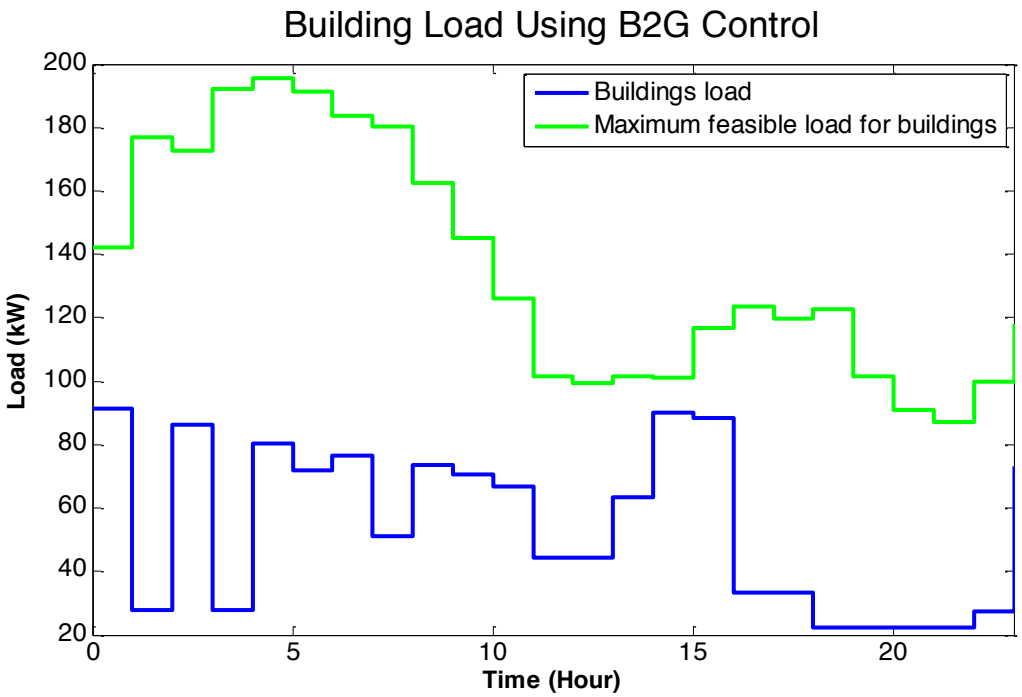

Figure 4.11: Load profile results from simulation using tuned B2G control.

Using the B2G control mode, the building load stays under the feasible load allowed by the grid. This shows the advantage of considering load factor in the objective function compared to price control. Price control does not directly consider this constraint, so may violate the maximum feasible load.

Figure 4.12 illustrates the difference in using the B2G objective function. Since price is considered in the objective function, the controller uses more power at times when the price is low. Comparing to price control, power load is distributed more evenly over these hours. This means that the price increases, but the more even distributed load increases load factor. This comprise is the general idea behind the B2G index.

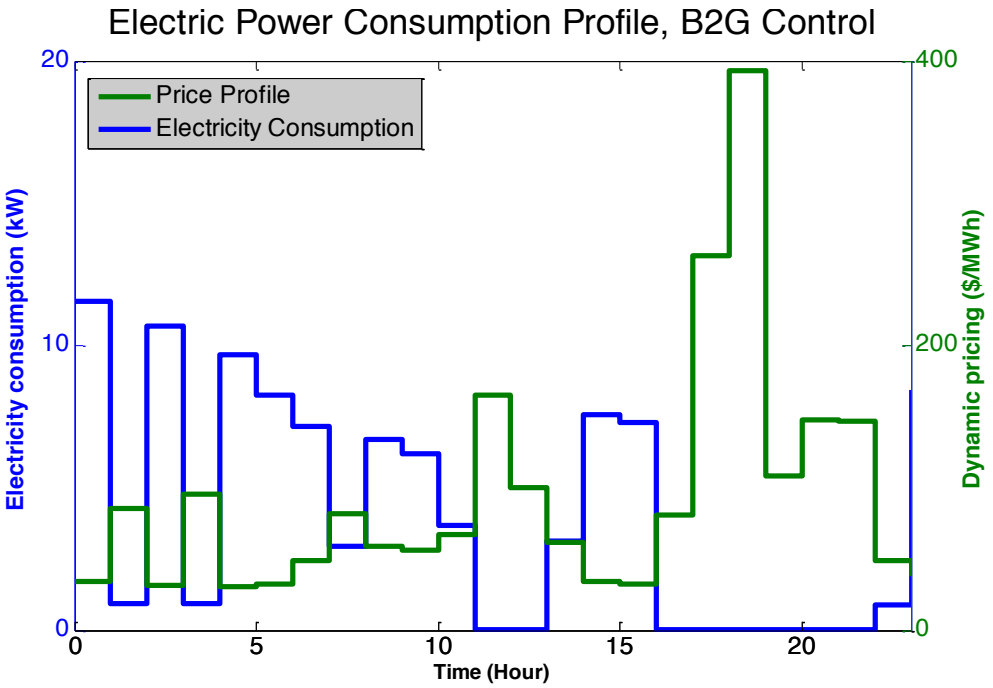

Figure 4.12: Electricity consumption results from simulation using tuned B2G control

4.5 Objective Function Comparison

The following figures compare three objective functions: price control, load factor control, and the B2G index. The compromise provided by the B2G index is clear. A balance is found between prioritizing price and load factor, and both the consumer and grid distributor benefit.

Figure 4.13 shows a comparison of the load profiles under price control, B2G control, and load factor control. The load factor control shows a relatively flat load. There are very large spikes in the price control load, corresponding to hours with cheap power. The B2G controller shows a compromise between these. There is more variation in the load than in the load factor load profile, but it eliminates the large spikes that occur when load factor is not considered at all.

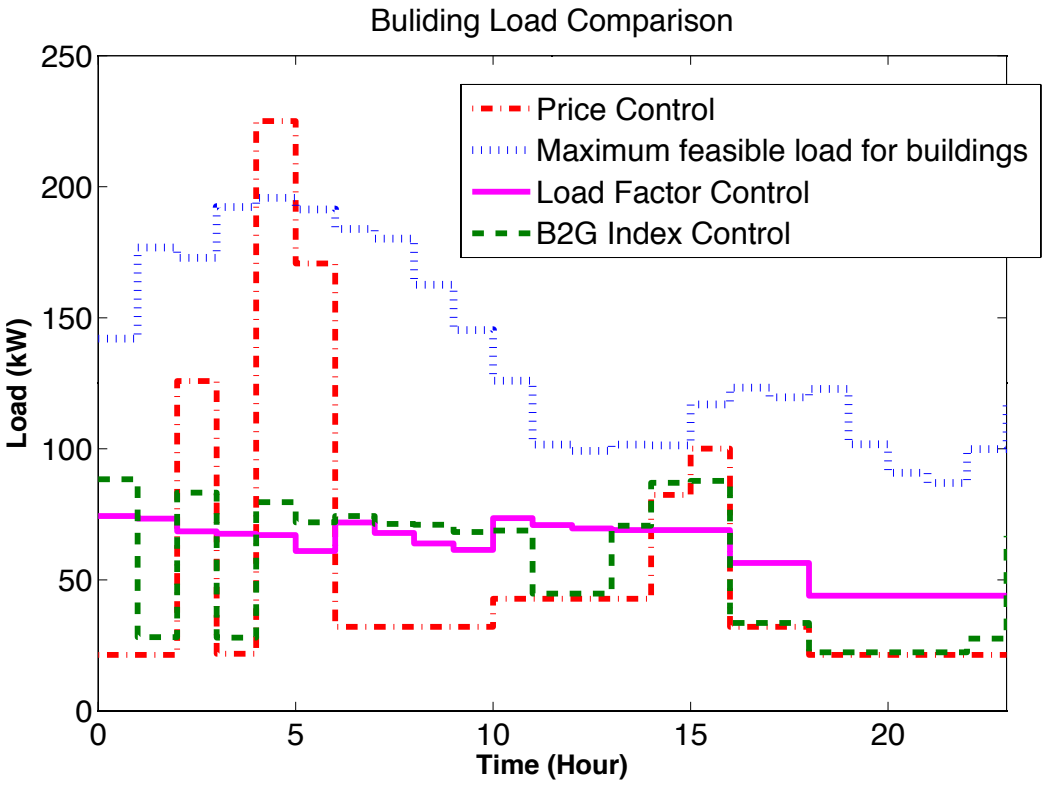

Figure 4.13: Comparison of load profiles with three different MPC controllers

Figure 4.14 shows a comparison of the HVAC run cost under price control, B2G control, and load factor control. The load factor controller does not consider price, so cost becomes large during the hours when price is large. The price controller only uses power during hours where the cost is very low. The B2G controller shows a compromise between these. The heating schedule is more evenly distributed over time than in price control, since price is still considered, the electrical consumption becomes small during hours with relatively high price.

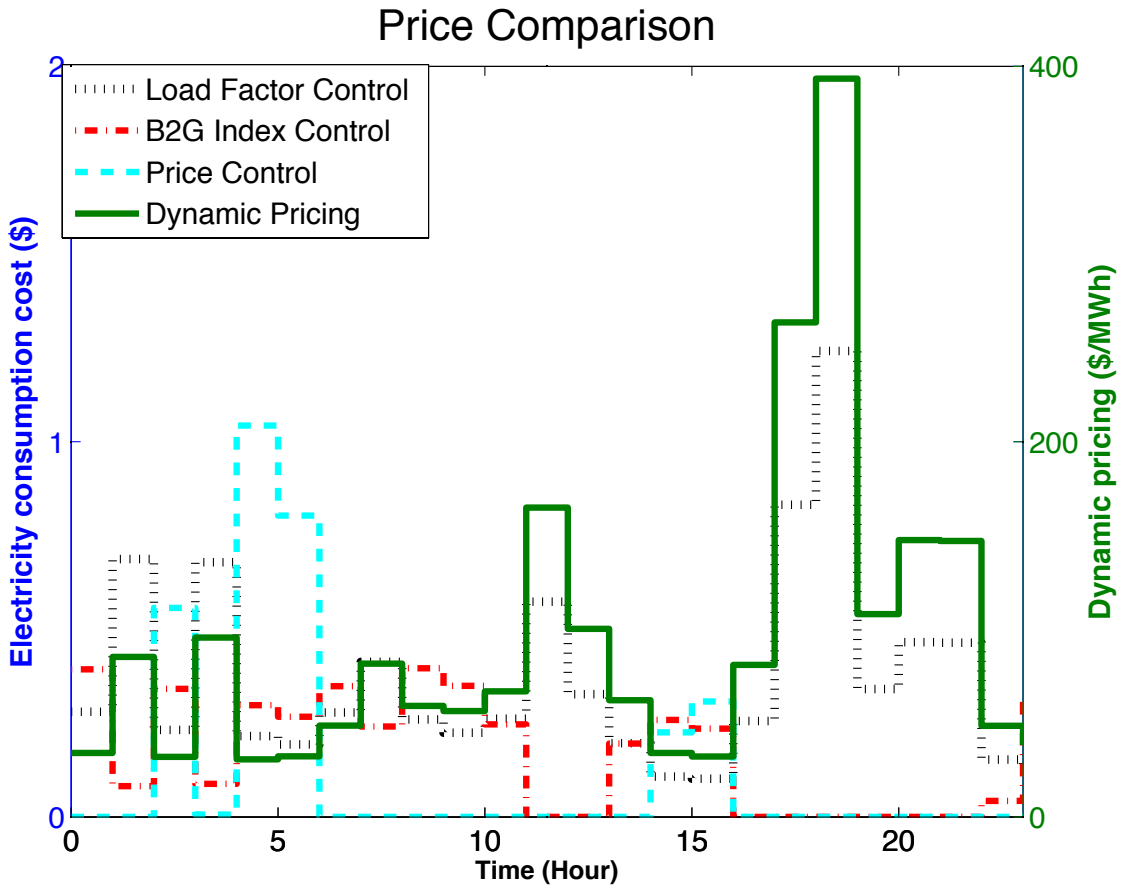

Figure 4.14: Comparison of cost of electricity consumption for three different MPC controllers

Using the B2G control mode has multiple benefits for the system performance. The system shows price and energy savings compared to rule-based or load factor control, which benefit the consumer. The system also avoids the large spikes in the hourly power consumption which are present during the price control mode, which benefits the grid distributor. This balance makes B2G optimization an attractive option for both consumer and power grid distributor.

Chapter 5

5 Conclusions and Future Work

5.1 Conclusions

The goal of this study was to design MPC algorithms to control building HVAC systems in a smart grid environment. Building HVAC systems account for a large portion of U.S. energy consumption. Using an MPC control algorithm allows to building to leverage aspects of Smart Building and Smart Grid technology to increase efficiency, benefiting both the consumer and the grid as a whole.

First, the objective was to design a control algorithm which minimized the cost of running the HVAC system. This method relys on foreknowledge of the hourly dynamic price of power.

Three different scenarios of MPC were considered for price minimization. The control variables for actuating the HVAC system varied between each of the three scenarios. These were mass flow rate control, supply temperature control, and combined mass flow rate and supply temperature control. The results show that all cases of MPC have performance advantages over rule-based control. Under dyanmic pricing, the performance of the system increased by at least 39% under all three control modes, when compared to the RBC. Combined supply temperature and mass flow rate control shows the best performance out of the three MPC control modes in all scenarios. Combined mass flow rate and supply temperature control had a performance increase of 2% over supply temperature contol, and a performance increase of 13% over mass flow rate control.

These results show that the extra control variable available in the combined mass flow rate and supply temperature control case leads to a lower cost result from the optimization. This is because the actuator is stronger during hours when the cost of power is low.

Next a battery storage model was integrated into the smart building simulation. The model for the battery was developed and placed into the dynamics of the optimization problem. These results show that there is an increase in system performance of .6% when battery storage is included, when compared to MPC

without battery storage. When compared to RBC, the MPC controller with battery storage showed performance increases of over 50%. The system is expected to show even further gains if a battery with SOC charateristics designed for building energy usage were applied to the problem.

Next, the objective function was changed from price optimization to energy optimization. The goal was to minimize the amount of energy used by the HVAC system. Once again, mass flow rate control, supply temperature control, and combined supply temperature and mass flow rate control were compared. Under flat pricing, the performance of all three MPC control modes exceed that of the RBC by over 30%. These results show that the advantage of having more control over the system extends to this case with an energy cost function. The extra actuation flexibility afforded the system leads to stronger performance. All MPC cases compared favorably to the on-off controller, showing the general advantage of optimal model-based control over more traditional control methods for BEMS.

The scope of the project was further expanded by considering the Smart Building as a node in a Smart Grid environment. The previous price and energy optimization has clear benefits in cost savings and energy efficiency from the perspective of a power consumer. By considering factors such as the peak energy usage, the optimization can benefit both the power consumer and the grid operator.

The optimization problem was formulated to minimize the load factor. These results showed that using MPC allowed for the building to use a much more balanced amount of energy hour to hour, compared to the traditional controller. This flat load profile benefits the power grid.

Finally, an optimization problem was formulated to benefit both the grid operator and energy consumer. In B2G control, the objective is to minimize a weighted average of the price of power and the building's load factor. Weights for this objective function were chosen through a tuning process. The results showed that using the B2G objective function for MPC showed benefits when compared to using the run cost objective function. The B2G controller was able to stay within load constraints for the system, while the price contoller was not. The B2G control found a balance between price optimization and load factor optimization which benefitted both sides. Large peaks were eliminated from the power load, and the profile was still scheduled in a way which avoiding power draw during hours with a very high price. When comparing the three control modes of supply temperature control, mass flow rate control, and combined mass flow rate and supply temperature control

when applied to B2G control, combined mass flow rate and supply temperature control had the best performance. Combined mass flow rate and supply temperature control had a 1.7% performance increase over supply temperature control and a 20% performance increase over mass flow rate control.

5.2 Future Work

There are interesting ways this work may be expanded upon in the future. The most revlavent extensions focus on additional work using energy storage systems and an experimental validation of the simulated results.

The battery storage system showed a small increase in performance during price optimization. It may be that larger gain could be found by changing the type of battery modeled. The battery chosen may not be the most optimal for the building energy storage scenario. A higher capacity battery would likely allow for further increases in performance. These simulations with an updated battery model would be one extension of this work.

The building to grid optimization results could also be expanded on. The battery storage model could be implemented in this scernario. The B2G index optimization with battery storage could be compared to the optimization without battery storage to see how the addition of the battery system could benefit the grid as a whole.

Finally, the results of this study could be experimentally validated. The thermal model used has been experimentally validated. The next step is to implement the control logic in real-time in an actual Smart Building.

References

[1] "DOE Building Energy Data Book," http://buildingsdatabook.eren.doe.gov/TableView.aspx?table=1.1.4, 2013. Accessed August 20, 2015.

[2] S. Tiptipakorn and W. Lee. “A Residential Consumer-Centered Load Control Strategy in Real-Time Electricity Pricing Environment”. *39th North American Power Symposium*: 505-510, 2007.

[3] K. Fong and V. Hanby, and T.T. Chow. “HVAC system optimization for energy management by evolutionary programming”. *Energy and Buildings,* 38(3): 220-231, 2006

[4] M. Muratori, M, V. Marano, R. Sioshansi, and G. Rizzoni. "Energy consumption of residential HVAC systems: A simple physically-based model". *Power and Energy Society General Meeting 2012*, 1(8): 22-26, 2012.

[5] Z. Liao and A. Dexter. “A simplified physical model for estimating the average air temperature in multi-zone heating systems”. *Building and Environment*, 39(9): 1013-1022, 2004.

[6] W. Cai, Y. Soh, L. Xie, and S. Li, “HVAC system optimization—condenser water loop”. *Energy Conversion and Management*, 45(4): 613-630, 2004.

[7] M. Risbeck, C. Maravelias, J. Rawlings, and R. Turney. "Cost optimization of combined building heating/cooling equipment via mixed-integer linear programming". *American Control Conference 2015,* 1(3): 1689-1694, 2015

[8] P. Samadi, A. Mohsenian-Rad, R. Schober, V. Wong, and J. Jatskevich. "Optimal Real-Time Pricing Algorithm Based on Utility Maximization for Smart Grid". *First IEEE International Conference on Smart Grid Communications 2010, 4(6):415-420,* 2010.

[9] P. Nyeng and J. Ostergaard. "Information and communications Systems for Control-by-Price of Distributed Energy Resources and Flexible Demand". *IEEE Trans. Smart Grid*, 2(2):334-341, 2011.

[10] Ning Lu. "Design considerations of a centralized load controller using thermostatically controlled appliances for continuous regulation reserves". *IEEE Power and Energy Society General Meeting 2013*, 1(1):21-25, 2013.

[11] H. Kim and M. Zhu. "Distributed robust frequency regulation of smart power grid with renewable integration". *American Control Conference 2015*, 1(3): 2347-2352, 2015.

[12] K. Hirata, J. Hespanha, and K. Uchida. "Real-time pricing and distributed decision makings leading to optimal power flow of power grids". *American Control Conference 2015*, 1(3): 2284-2291, 2015.

[13] H. Huang, L. Chen, and E. Hu. "A hybrid model predictive control scheme for energy and cost savings in commercial buildings: Simulation and experiment". *American Control Conference 2015*, 1(3): 256-261, 2015.

[14] M. Vasak, A. Starcic, and A. Martincevic. "Model predictive control of heating and cooling in a family house". *MIPRO Proceedings of the 34th International Convention 2011*, 23(27): 739-743, 2011.

[15] M. Maasoumy, M. Razmara, M. Shahbakhti, and A. Sangiovanni Vincentelli. "Handling model uncertainty in model predictive control for energy efficient buildings". *Energy and Buildings*, 77: 377-392, 2014.

[16] M. Razmara, G. Bharati, M. Shahbakhti, S. Paudyal, and R. Robinett. "Bidirectional optimal operation of smart building-to-grid systems,"*American Control Conference 2015*, 1(3): 288-293, 2015.

[17] M. Maasoumy and A. Sangiovanni-Vincentelli. "Total and Peak Energy Consumption Minimization of Building HVAC Systems Using Model Predictive Control". *IEEE Design & Test of Computers*, 29(4): 26-35, 2012.

[18] T. Wei, Q. Zhu, and M. Maasoumy. "Co-scheduling of HVAC control, EV charging and battery usage for building energy efficiency". *IEEE/ACM International Conference on Computer-Aided Design 2014*, 2(6): 191-196, 2014.

[19] M. Galus, S. Koch, and G. Andersson. "Provision of Load Frequency Control by PHEVs, Controllable Loads, and a Cogeneration Unit". *IEEE Transactions on Industrial Electronics,* 58(10), 4568-4582, 2011.

[20] M. Nowak and A. Urbaniak. "Utilization of intelligent control algorithms for thermal comfort optimization and energy saving". *12th International Carpathian Control Conference 2011, 25(28): 270-274,* 2011.

[21] R. Halvgaard, N. Poulsen, H. Madsen, and J. Jorgensen. "Economic Model Predictive Control for building climate control in a Smart Grid". *IEEE PES Innovative Smart Grid Technologies 2012*, 1(6):16-20, 2012.

[22] J. Rehrl and M. Horn. "Temperature control for HVAC systems based on exact linearization and model predictive control". *IEEE International Conference on Control Applications 2011*, 28(30): 1119-1124, 2011.

[23] A. Kelman, Y Ma, and F. Borrelli, "Analysis of local optima in predictive control for energy efficient buildings". *50th IEEE Conference on Decision and Control and European Control Conference 2011*, 12(15): 5125-5130, 2011.

[24] Y. Ma, F. Borrelli, B. Hencey, B. Coffey, S. Bengea, and P. Haves. "Model Predictive Control for the Operation of Building Cooling Systems," *IEEE Transactions on Control Systems Technology,* 20(3): 796-803, 2012.

[25] M. Paranjape. "Optimal Control of Buiding Energy With Smart-Grid Interaction". Master's thesis, Michigan Technological University, 2014.

[26] *5Kwhr Air Cooled Battery Product Manual.* LG Chem.

[27] J. Löfberg. "YALMIP : A Toolbox for Modeling and Optimization in MATLAB*"*. Proceedings of the CACSD, 2004.

[28] A. Wächter and L Biegler. "On the Implementation of a Primal-Dual Interior Point Filter Line Search Algorithm for Large-Scale Nonlinear Programming". *Mathematical Programming* 106(1), 25-57, 2006.

[29] *2012 ASHRAE handbook. Heating, Ventilating, and Air Conditioning Systems and Equipment.* American Society of Heating, Refrigerating, and Air Conditioning Engineers. 2012.

Appendix A State Space Model

The matrices for the state space model developed in section 2.3 are shown in full below.

$$A = \begin{matrix} -4 * \frac{x_1}{C^w R^w} & \frac{1}{C_r \times R_w} & \frac{1}{C_r \times R_w} & \frac{1}{C_r \times R_w} & \frac{1}{C_r \times R_w} \\ \frac{1}{C_w \times R_w} & \frac{2}{C_w \times R_w} & 0 & 0 & 0 \\ \frac{1}{C_w \times R_w} & 0 & \frac{2}{C_w \times R_w} & 0 & 0 \\ \frac{1}{C_w \times R_w} & 0 & 0 & \frac{-2}{C_w \times R_w} & 0 \\ \frac{1}{C_{w51} \times R_{w51}} & 0 & 0 & 0 & -\left(\frac{1}{C_{51}^w R_{51_1}} + \frac{1}{C_{51}^w R_{51_5}}\right) + \frac{1}{C_{51}^w R_{51_5}} \end{matrix}$$

$$B = \begin{matrix} \frac{1}{C_r \, \dot{m} \, C_p} \\ 0 \\ 0 \\ 0 \\ 0 \end{matrix}$$

$$F = \begin{matrix} 0 & 0 & 0 & \frac{1}{C_r \times R_{win}} \\ \frac{1}{C_r \times R_w} & 0 & 0 & 0 \\ 0 & \frac{1}{C_r \times R_w} & 0 & 0 \\ 0 & 0 & \frac{1}{C_r \times R_w} & 0 \\ 0 & 0 & 0 & \frac{1}{C_r \times R_w} \end{matrix}$$

$$C = [1 \quad 0 \quad 0 \quad 0 \quad 0]$$

Appendix B Thesis Files Summary

The following files were used to prepare this thesis.

Table B.1: MATLAB Simulation Files

File Name	Description
RBC.m	Rule based controller simulation
TempContPrice.m	Price optimization with temperature control

MassContPrice.m	Price optimization with mass flow rate control
NonlinContPrice.m	Price optimization with combined mass flow rate and temperature control
ESSPriceMPC.m	Price optimization with battery energy storage model added to HVAC system
TempContEng.m	Energy optimization with temperature control
MassContEng.m	Energy optimization with mass control
NonlinContEng.m	Energy optimization with combined mass flow rate and supply temperature control
LoadFactorMPC.m	Load Factor optimization with combined mass flow rate and supply temperature control
B2GMPC.m	Building to Grid index optimization

Table B.2: Input Data Files

File Name	Description
SI-DataSheet.xls	Sensor outdoor temperature data from Feburary 2012 used as input to model.
Dynamic_Pricing.xls	Dynamic Pricing Profile
Base_Load.xls	Base power load of the building, added to HVAC load
Power.xls	Maximum allowable power load for each

	node in grid
Power_LF.xls	System load Factor

Table B.3: Date Output Files

File Name	Description
MassFlowTune.xls	Tuning data for supply temperature control.
SupplyTempTune.xls	Tuning data for mass flow rate control

Table B.4: MATLAB Figure Files

File Name	Description
RBCTempProf.fig	Figure 3.1
RBCPowerComp.fig	Figure 3.2
TempPriceTempProl.fig	Figure 3.4
TempPriceInputs.fig	Figure 3.5
MassPriceTempProf.fig	Figure 3.7
MassPriceInputs.fig	Figure 3.8

NonlinPriceTempProf.fig	Figure 3.9
NonlinPriceInputs.fig	Figure 3.10
NonlinPricePower.fig	Figure 3.11
NonlinPriceCost.fig	Figure 3.12
PriceContComparePower.fig	Figure 3.13
PriceContComparePrice.fig	Figure 3.14
ESSEnergyFlow.fig	Figure 3.16
ESSPower.fig	Figure 3.17
ESSBattSOC.fig	Figure 3.18
EnergyCompare.fig	Figure 3.19
LoadViolation.fig	Figure 4.1
LFContTempProf.fig	Figure 4.3
LFContPower.fig	Figure 4.4
PriceLFLoadCompare.fig	Figure 4.5
PriceLFCostCompare.fig	Figure 4.6
TunePrice.fig	Figure 4.7
TuneLF.fig	Figure 4.8
TuneB2G.fig	Figure 4.9
B2GtempProf.fig	Figure 4.10
B2GloadProf.fig	Figure 4.11
B2Gpower.fig	Figure 4.12
CompareB2Gload.fig	Figure 4.13
CompareB2GPrice.fig	Figure 4.14

Table B.5: Image Files

File Name	Description
Lakeshore.jpg	Figure 2.1
SystemSchem.png	Figure 2.2
RCmodel.png	Figure 2.3
HVACSys.png	Figure 2.4
ModelValidation.jpg	Figure 2.5
MPC.png	Figure 2.6

PowerMap.jpg	Figure 2.7
SupplyTempControlMassTune.jpg	Figure 3.3
MassControlTempTune.jpg	Figure 3.6
SmartGrid.jpg	Figure 4.2